The impact of passive social media viewers in influence maximization

Michael Kahr[1], Markus Leitner[2] and Ivana Ljubić[3]

[1]University of Graz, Institute of Operations und Information Systems, Graz, Austria. michael.kahr@uni-graz.at
[2]Vrije Universiteit Amsterdam, Departnment of Operations Analytics, Amsterdam, Netherlands. m.leitner@vu.nl
[3]ESSEC Business School, Department of Information Systems, Decision Sciences and Statistics, Paris, France. ivana.ljubic@essec.edu

February 2, 2024

Abstract

A frequently studied problem in the context of digital marketing for online social networks is the influence maximization problem that seeks for an initial seed set of influencers to trigger an information propagation cascade (in terms of active message forwarders) of expected maximum impact. Previously studied problems typically neglect that the probability that individuals passively view content without forwarding it is much higher than the probability that they forward content. Considering passive viewing enables to maximize more natural (social media) marketing metrics including: (a) the expected organic reach, (b) the expected number of total impressions, or (c) the expected patronage; all of which are investigated in this paper for the first time in the context of influence maximization. We propose mathematical models to maximize these objectives whereby the model for variant (c) includes individual's resistances and uses a multinomial logit model to model customer behavior. We also show that these models can be easily adapted to a competitive setting in which the seed set of a competitor is known. In a computational study based on network graphs from Twitter, now X, (and from the literature) we show that one can increase the expected patronage, organic reach, and number of total impressions by 36% on average (and up to 13 times in particular cases) compared to seed sets obtained from the classical maximization of message forwarding users.

Keywords: Influence maximization, social networks, generalized Benders decomposition

1 Introduction

Online social networks have evolved to crucial communication channels used by stakeholders such as individuals, companies, or political parties. They are commonly used in online marketing campaigns that propagate information related to products or political candidates and can be more effective than traditional campaigns [62]. Nowadays, the influencer marketing industry is an important pillar of the marketing mixes of companies and its worth is estimated up to $16.4 billion in 2022 [16]. A reason of this trend is that such campaigns ease to exploit *social influence* effects, which may cause individuals to adjust their opinions based on the opinions of their peers, to stimulate certain consumer decisions [37], or to sway political election outcomes [5]. Influencer marketing campaigns can also reach individuals who use ad blockers. The relative number of such users is 42.7 % of the global (16-64 years old) internet-using population [9].

The decentralized spread of information in social networks such as (fake) news, opinions, or advertisements is often referred to as *influence propagation*. Influence cascades are typically triggered by so-called *seed nodes* such as *influencers* that are commonly incentivized by external means such as remunerations or product discounts. In order to increase expected sales or simply awareness, a common objective is to maximize the (expected) number of reached network participants (*nodes*). The classical variant of the underlying *influence maximization problem* (IMP) was introduced by Kempe et al. [29]. Since then, (variants of) the IMP have been intensively studied by researchers from the computer science and operations research communities. IMPs seek for a seed set of network nodes that trigger an influence cascade of maximum impact and which is typically constrained by cardinality or available budget, see, e.g., Nguyen and Zheng [46]. Several models of the influence propagation process have been studied; see Singh et al. [57] for a recent comprehensive survey. The majority of the works related to IMPs use either the *linear threshold model* based on Granovetter [19] or the probabilistic *independent cascade model* as used by Kempe et al. [29]. The latter authors showed that the IMP is NP-hard under these two propagation models and that the objective function is submodular. Thereby, they triggered the development of several $1 - {}^{1}\!/_{e}$ approximation algorithms (see, e.g., Banerjee et al. [2] and the references therein) based on the seminal work of Nemhauser et al. [44]. Here, e denotes the base of the natural logarithm. IMPs were further tackled with heuristic methods that employ topological network metrics such as betweenness centrality, however, without providing approximation guarantees (e.g., Liu et al. 40, Wasserman et al. 65). Several recent articles tackle IMP variants with exact solution methods based on *integer linear programming* (ILP). The majority of them use (variants of) the linear threshold model, see, e.g., Fischetti et al. [13], Günneç et al. [21, 22], Raghavan and Zhang [50, 51, 53, 52]. In contrast, only very few exact solution methods have been proposed for variants of the IMP using the probabilistic independent cascade model. These include Güney et al. [20] and Wu and Küçükyavuz [66] for the classic IMP variant, and Farnad et al. [12] who address aspects related to algorithmic bias, fairness and equity in their work on fairness-aware influence maximization. Recently, there is also a growing interest in different variants of the competitive influence maximization problem (CIMP) in which more than one influence-spreading entity is considered, see, e.g., Bharathi et al. [4], Carnes et al. [6], Kahr et al. [25], Keskin and Güler [31], Lin and Lui [39], Song et al. [58], Tanınmış et al. [61].

1.1 Motivation for and novelties of our model

The next paragraphs discuss shortcomings of existing (C)IMPs addressed in this article.

Active nodes versus organic reach, and total impressions. Existing methods focus on maximizing the number of so-called *active nodes*. These are nodes which exert influence on their peers by *forwarding* content to them after being successfully influenced by (one of) their active neighbors. It was shown, however, that the probabilities that users only view content in their newsfeed are notably larger than the probabilities that they also forward the content [11, 64], and that the vast majority of influence cascades terminates after one hop [17]. We thus extend the existing influence events by *passive viewing events* meaning that nodes view content without forwarding it. Note that we explicitly use the term *passive* here to distinguish from viewing events at node activation (i.e., people typically also view content before they share it). This enables to consider three new objective functions corresponding to (social media) marketing metrics which are of great interest in that field, and which have been neglected in (C)IMPs so far. The first one is the *organic reach* which refers to nodes that viewed the content of a specific marketing campaign in their newsfeed at least once. In contrast, the term *total impressions* refers to the total number of views including multiple views of one and the same content at one and the same node, e.g., an advertisement appearing more than once in a node's newsfeed. Another important marketing metric is the so-called *patronage* which we introduce in the context of IMPs in the next paragraphs.

Node resistance. We assume that the strength of influence on a node (e.g., its responsiveness to an advertisement) is directly correlated with the number of impressions triggered by its peers and inversely correlated with its *resistance*. That is, individuals may be resistant to some content meaning that, despite viewing it many times, they will probably never be convinced of it. The extent of a node's resistance (or, conversely, responsiveness) can be estimated using, for instance, observable parts of demographic, psychographic or sociographic factors or by analyzing the content users produce such as hashtags or more detailed text analysis [34, 33]. The impact of such resistances could be partly considered in traditional (C)IMP variants by, e.g., infinite thresholds in propagation models based on thresholds or zero activation probability in cascade models. This would, however, rule out the consideration of resistant nodes that forward information they consider to be of interest to their peers in an altruistic manner. Our model overcomes this limitation through the consideration of explicit resistance values associated to nodes.

Customer choice behavior. An implicit assumption in the aforementioned (C)IMP variants is that active nodes *patronize* the influence spreading entity, e.g., adopt an advertised product or opinion. When it comes to customer choice behavior, however, it is widely accepted that customers prefer options that maximize their individual utilities. Customer choice behavior is frequently modeled with random-utility *multinomial logit* (MNL) models (see, e.g., McFadden 43, Swait and Louviere 60). One advantage of such models is that they allow a mapping between (un)observed customer characteristics and individual preferences over a set of alternatives (e.g., products). The term preference here means the probability that a certain alternative is chosen and it is also called *patronizing-probability* or simply *patronage*. The uncertain unobserved parts of the customer characteristics are typically modeled as random variables that are independent and identically distributed following a Gumbel distribution; see Baltas and Doyle [1] for an introductory survey.

The (discrete choice) models proposed in this article enable to focus on the organic reach or total impressions while maximizing one of the following metrics. The first three of these metrics are studied for the first time in this article to the best of our knowledge:

(a) the expected *organic reach* (from now on referred to as the variant `O`),

(b) the expected number of *total impressions* (the variant `T`),

(c) the expected *patronage* of the organic reach (the variant `R`),

(d) the expected number of *message forwarders*, i.e., active nodes (the variant `F`).

1.2 Scientific contribution and outline

As discussed above, only very few articles have proposed ILP-based exact solution algorithms for (C)IMPs and we are not aware of approaches considering MNL models or passive viewing events in (C)IMPs. The contributions of this article are summarized as follows:

- We define three new IMP variants based on an adapted independent cascade (IC) model in the spirit of Kempe et al. [29]. Variant `R` maximizing the expected patronage is the most general one and it includes all novelties mentioned above (i.e., an MNL-based objective function incorporating node views, node resistance, and customer choice behavior). We show that minor manipulations to this variant allow to optimize different metrics, i.e., the expected organic reach (`O`), expected number of total impressions (`T`) or expected number of active nodes (`F`) (the latter being the classical IMP in the spirit of 29). We further show that all three new problem variants are NP-hard, that the precise evaluation of these objective functions is #P-hard, and that all three new objective functions are submodular, but non-monotone.
- We propose a mixed-integer (non)linear program (MI(N)LP) for the three new IMP variants, prove the existence of an exact linearization based on *generalized Benders decomposition* [15], and show how to separate the generalized Benders cuts in polynomial time. As an alternative, we also consider a linearization based on outer approximation [10].
- We derive worst-case bounds for the greedy marginal gain heuristic for solving the proposed IMP variants in the spirit of Nemhauser et al. [44].
- Our benchmark instances based on real data are extracted via the development interface of Twitter by querying information of users, tweets, and their relation to each other. Specific hashtags are chosen as examples which can be used to promote products or events.
- The results of our computational study show that: (i) our models outperform state-of-the-art heuristics in terms of the quality of objective values; (ii) one can increase the expected organic reach, the expected number of total impressions, and the expected patronage by 36% on average (and up to 13 times in particular cases) by considering our models instead of the classical IMP [29]; (iii) message forwarding cascades are short on average which emphasizes the importance of considering passive viewing events.
- Finally, we show that all our models and algorithms can be easily adapted to a CIMP with static competition.

The article is organized as follows: The problem is defined and structural properties are studied in Section 2; Mathematical models are given in Section 3; Worst-case bounds are derived, and heuristics are discussed in Section 4; The generation of real-world instance graphs from Twitter is discussed in Section 5; Our algorithmic framework is presented in Section 6, and computational results are provided in Section 7; Conclusions are given in Section 8; Proofs of all theoretical results and additional results are given in the appendices.

2 Problem definition

The considered IMP variants are defined on a simple directed graph $G = (V, A)$ modeling a social network. Node set V represents the network participants and arc set $A \subseteq V \times V$ their relations. Forwarding and viewing probabilities $p^{\mathrm{f}}_{ij} \in [0,1]$ and $p^{\mathrm{v}}_{ij} \in [0,1]$, respectively, are associated with each arc $(i,j) \in A$. The former represent the probabilities that an inactive node j will be activated by an *active* neighbor i, i.e., node j *views and forwards* content received from i. The latter represent the probabilities that node j *only views* content received from an active neighbor i (without forwarding it). Note that we assume that active nodes always view content before forwarding it and that $0 \leq p^{\mathrm{f}}_{ij} \leq p^{\mathrm{v}}_{ij} \leq 1$ holds for each $(i,j) \in A$; cf., Section 2.1 for details on the influence propagation process. The objective is to identify a seed set $S^* \in V$ of at most $k \in \mathbb{N}$ nodes that maximizes an objective function $\sigma_{\mathtt{M}}(S)$, i.e.,

$$S^* \in \operatorname*{argmax}_{S \subseteq V, |S| \leq k} \ \sigma_{\mathtt{M}}(S)\,, \tag{1}$$

where $\sigma_{\mathtt{M}}(S)$ measures the impact of a marketing campaign with respect to metric $\mathtt{M} \in \{\mathtt{O}, \mathtt{T}, \mathtt{R}, \mathtt{F}\}$. The considered metrics include the expected organic reach ($\mathtt{O}$), the expected number of total impressions ($\mathtt{T}$), expected patronage ($\mathtt{R}$), and the expected number of message forwarders ($\mathtt{F}$); see Section 2.3. In the variant $\mathtt{R}$, additional *resistance values* $r_i \in \mathbb{R}_{>0}$ are associated to nodes $i \in V$. They are used to account for the fact that influenced nodes do not necessarily need to adopt a (promoted) content, cf. Section 1. Note that we define the resistance vector $\mathbf{r} \in \mathbb{R}^{|V|}_{>0}$ on the positive orthant for technical reasons. The vector coordinates may, however, be arbitrary small.

2.1 Adapted independent cascade (IC) model

In order to evaluate functions $\sigma_{\mathtt{M}}(\cdot)$, an influence propagation process needs to be modeled. To this end, we propose an IC model which augments the classical one [29] by viewing probabilities. As the classical IC model, it assumes that only the seed nodes from set S are initially active (and trigger a propagation process), all other nodes are initially inactive, and that each node can get activated only once. In contrast, nodes can view content multiple times (at most once from each active in-neighbor). During the propagation process, each active node i tries to influence each of its neighbors j, $(i,j) \in A$, exactly once, and these attempts are independent from each other. An attempt of node i to influence neighbor j results in one of the following three outcomes: (i) If j is inactive, it may become active (which happens with probability p^{f}_{ij}) and starts trying to influence its neighbors by sharing the content. Note that changing j's state from inactive to active implies that j also views the content (since $p^{\mathrm{f}}_{ij} \leq p^{\mathrm{v}}_{ij}$) and, therefore increases its number of impressions by one. (ii) Node j (either inactive or already active) only views the content (which happens with probability p^{v}_{ij}) in which case its number of impressions is increased by one. (iii) Node j does not view the content (which happens with probability $1 - p^{\mathrm{v}}_{ij}$). The propagation process stops when there are no more active nodes that did not yet share the content with their neighbors.

Discrete influence scenarios. In the following we consider a discrete set of (all) influence propagation scenarios Ω instead of explicitly considering forwarding and viewing probabilities, p^{f}_{ij} and p^{v}_{ij}, respectively. The idea originates from Kempe et al. [29] who observed that the event that node i successfully activates node j, $(i,j) \in A$, can be interpreted as the outcome of a random coin-flipping event biased by p^{f}_{ij}. In this case, the authors declare arc $(i,j) \in A$ as *live*. Repeating

Figure 1: Illustration example of an instance graph, a scenario graph, and an influence propagation cascade.

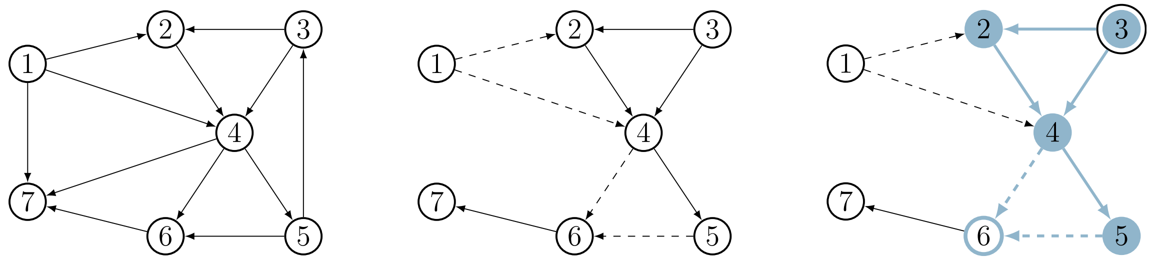

(a) Instance graph G (b) Scenario graph G^1 (c) Propagation in G^1

Note. Solid arcs in (b) and (c) correspond to activation arcs $\underline{A}^1$ and dashed arcs to viewing arcs $A^1 \setminus \underline{A}^1$.

the coin-flipping procedure for each arc $(i, j) \in A$ independently, yields an *influence scenario* $\omega \in \Omega$ which can be represented as a *scenario graph* $G^\omega = (V, A^\omega)$ containing only arcs that are live in scenario ω. One benefit of this approach is that the time aspect of the propagation process becomes irrelevant (although the activation process evolves dynamically over time) because it only matters *if* a node j can be activated in a certain influence scenario $\omega \in \Omega$. This is the case if there exists a path from some seed node $i \in S$ to node j in scenario graph G^ω. We augment the idea of Kempe et al. [29] with viewing probabilities p^{v}_{ij}, and discriminate live arcs $A^\omega \subseteq A$ in *activation arcs* $(i, j) \in \underline{A}^\omega \subseteq A^\omega$ (along which node i can activate node j), and *viewing arcs* $(i, j) \in A^\omega \setminus \underline{A}^\omega$ (along which node i can increase the number of j's impressions by one without activating it). Thus, in each scenario $\omega \in \Omega$ an arc $(i, j) \in A$ is represented either by (i) a forwarding arc in $\underline{A}^\omega$, (ii) a viewing arc in $A^\omega \setminus \underline{A}^\omega$, or (iii) is not included in A^ω. Consequently there exist $|\Omega| = 3^{|A|}$ possible realizations of scenario graphs G^ω. Further details about our adapted coin-flipping procedure are given in Section 6.2.

Figure 1 illustrates an instance graph (Figure 1a) for which we omit introducing precise influence probabilities p^{f}_{ij} and p^{v}_{ij}, a scenario graph $G^1 = (V, A^1)$ (Figure 1b), and an influence propagation cascade in G^1 (Figure 1c). Solid arcs in Figures 1b and 1c correspond to activation arcs $\underline{A}^\omega$ and dashed arcs to viewing arcs $A^\omega \setminus \underline{A}^\omega$. The exemplary influence spread (along blue, bold arcs) is given in Figure 1c and starts at seed set $S = \{3\}$. Active nodes are filled (blue), and viewing-only nodes are marked as bold. That is, nodes 2, 4 and 5 actively forward content triggered by (active) seed node 3 whereas node 6 only views the content. The number of impressions corresponds to the number of active in-neighbors in G^1. For instance, node 4 views the content twice via active in-neighbors 2 and 3, whereas node 5 views the content only once (via its active in-neighbor 4). Note that although node 4 has two in-going activation arcs (from nodes 2 and 3) it is activated only once (by definition) and that it does not matter whether its activated by node 2 or node 3. The second attempt to activate node 4 will simply increase its number of impressions to two. Node 6 also views the content twice, but is, however, not activated (as it has no in-going activation arc). Consequently, it does not forward the content to node 7. This example also illustrates that given a seed set S, the influence spread in a fixed scenario $\omega \in \Omega$ can be efficiently computed using *breadth-first-search* (BFS).

2.2 Set representation of the influence spread

To simplify notation, we define the following set-valued functions denoted by calligraphic capital letters, e.g., $\mathcal{F}(\cdot)$, for which we use notation $\mathcal{F}(i)$ if the argument is a singleton $\{i\}$ and assume that $\mathcal{F}(S)$ is equivalent to $\cup_{i \in S} \mathcal{F}(i)$ for node set $S \subseteq V$:

- The sets of in- and out-neighbors of node i in G^ω and G are denoted by $\mathcal{N}_\omega^-(i) = \{j : (j,i) \in A^\omega\}$, $\mathcal{N}_\omega(i) = \{j : (i,j) \in A^\omega\}$, $\mathcal{N}^-(i) = \{j : (j,i) \in A\}$, and $\mathcal{N}(i) = \{j : (i,j) \in A\}$, respectively.

- The *activation set* $\mathcal{A}_\omega(i)$ consists of all nodes reachable by activation arcs $\underline{A}^\omega$ from node i in scenario ω. For instance, $\mathcal{A}_1(3) = \{2,3,4,5\}$ in the example in Figure 1b. Note that set $\mathcal{A}_\omega(i)$ also contains node i by definition.

- The *reverse activation set* $\mathcal{A}_\omega^-(j)$ consists of all nodes that can activate a node j in scenario ω along forwarding arcs $\underline{A}^\omega$. For instance, $\mathcal{A}_1^-(5) = \{2,3,4,5\}$ in the example in Figure 1b.

- The *reachable set* $\mathcal{R}_\omega(i)$ consists of all nodes that view information propagated by i in scenario ω (at least once). For instance, $\mathcal{R}_1(3) = \{2,3,4,5,6\}$ in the example in Figure 1b. Note that set $\mathcal{R}_\omega(i)$ also contains node i, and that $\mathcal{A}_\omega(i) \subseteq \mathcal{R}_\omega(i)$.

- For each node $j \in V$, the number of impressions triggered by $S \subseteq V$ in scenario ω is given by the number of its active in-neighbors, i.e., $\nu_j^\omega(S) = |\mathcal{A}_\omega(S) \cap \mathcal{N}_\omega^-(j)|$.

2.3 Objective functions

This section defines the metrics used to measure the impact of a marketing campaign, discusses their submodularity properties, and the hardness of the resulting problem variants. First observe that we can express the objective function of (1) as

$$\sigma_{\mathtt{M}}(S) = \sum_{\omega \in \Omega} p^\omega \sigma_{\mathtt{M}}^\omega(S)\,, \tag{2}$$

where $0 < p^\omega < 1$ refers to the probability of (coin-flipping) scenario ω, and $\sigma_{\mathtt{M}}^\omega(S)$ denotes the objective function value for one specific scenario $\omega \in \Omega$ with respect to metric $\mathtt{M}$. For brevity we will only define functions $\sigma_{\mathtt{M}}^\omega(S)$ in this section. We also restrict seed nodes $i \in S$ from contributing to the objective function, which is of particular interest for metrics $\mathtt{T}$ and $\mathtt{R}$; see Remark 1 for the underlying reason and a clarifying example. For the sake of consistency, we keep that restriction also for variant $\mathtt{O}$ although it implies that the objective function is non-monotone; see Theorem 1 (and Remark 1).

Organic reach ($\mathtt{O}$). For a given scenario $\omega \in \Omega$ and seed set $S \subseteq V$, the number of nodes not in S that are reached in scenario ω, i.e., the *organic reach* in scenario ω, is defined by

$$\sigma_{\mathtt{O}}^\omega(S) = |\mathcal{R}_\omega(S) \setminus S|. \tag{3}$$

Theorem 1. *For any given $\omega \in \Omega$, function $\sigma_{\mathtt{O}}^\omega(S)$ is submodular, non-negative and non-monotone.*

Total impressions (T). For a given scenario $\omega \in \Omega$ and seed set $S \subseteq V$, the number of total impressions in scenario ω is given by

$$\sigma_{\mathtt{T}}^{\omega}(S) = \sum_{j \in V \setminus S} |\mathcal{A}_{\omega}(S) \cap \mathcal{N}_{\omega}^{-}(j)|. \tag{4}$$

For each node $j \in V \setminus S$, this function sums the number of active in-neighbors which corresponds to the content views of node j.

Theorem 2. *For any given $\omega \in \Omega$, function $\sigma_{T}^{\omega}(S)$ is submodular, non-negative and non-monotone.*

Expected patronage (R). A common assumption in decision theory is that individuals seek to maximize their own utility, based on their personal preferences and the attributes of the available alternatives. In the context of influence maximization, each individual can either patronize the distributed content or not, i.e., stay resistant. Each individual node $i \in V$ is assumed to maximize its own utility. Each single view of the propagated content increases the utility function by $\bar{b}_i + \bar{\epsilon}'_i$. Alternatively, the utility of "staying resistant" is $\bar{r}_i + \bar{\epsilon}''_i$. Here, $\bar{b}_i$, and $\bar{r}_i$ denote the deterministic parts of the utilities related to observable (demographic, sociological, psychometric) factors [34], whereas the ϵ-terms denote unobservable parts of the utilities, which are assumed to be independent and identically distributed following a Gumbel distribution. Then, for a given scenario ω, as shown in [42], the *probability* that node $j \in V$ patronizes the content triggered by seed set S is given by the MNL

$$\frac{\nu_j^{\omega}(S) e^{\bar{b}_j}}{\nu_j^{\omega}(S) e^{\bar{b}_j} + e^{\bar{r}_j}},$$

where $\nu_j^{\omega}(S)$ denotes the total number of impressions of node j. The term above can be simplified to

$$\frac{b_j \nu_j^{\omega}(S)}{b_j \nu_j^{\omega}(S) + r_j}, \tag{5}$$

where $b_j = e^{\bar{b}_j}$ and $r_j = e^{\bar{r}_j}$. Finally, the sum of these individual probabilities over all nodes $j \in V \setminus S$ is what we call the patronage, for given seed S under scenario ω, that is,

$$\sigma_{\mathtt{R}}^{\omega}(S) = \sum_{j \in V \setminus S} \frac{b_j \nu_j^{\omega}(S)}{b_j \nu_j^{\omega}(S) + r_j}. \tag{6}$$

Theorem 3. *For any given $\omega \in \Omega$, the objective function $\sigma_{\mathtt{R}}^{\omega}(S)$ is submodular, non-negative and non-monotone.*

Remark 1. Restricting seed nodes $i \in S$ from contributing to the objective functions avoids counting their impressions (triggered by themselves or other seed nodes), which could lead to unnatural seed set choices. Consider, for instance, the disconnected graph with two connected components in Figure 2, and assume that $p_{ij}^{\mathrm{f}} = p_{ij}^{\mathrm{v}} = 1$ for all $(i,j) \in A$, and $k = 1$. Observe that $|\mathcal{N}(i)| = |\mathcal{N}^{-}(i)| = 10$, and $|\mathcal{N}(j)| = 15$ whereas $\mathcal{N}^{-}(j) = \emptyset$. A natural seed set choice for variant T would be $\{j\}$ with $\sigma_{\mathtt{T}}(\{j\}) = 15$ reaching 15 non-seed nodes (with one impression each). This solution is only optimal if seed nodes do not contribute to the objective function. Otherwise, seed set $\{i\}$

with $\sigma_{\mathtt{T}}(\{i\}) = 20$ would be optimal which reaches only ten non-seed nodes (with one impression each) due to ten "self-impressions" of seed node i. Another consequence of restricting seed nodes from contributing to the objective function is that the latter is non-monotone. For instance, the optimal solution for $k = 2$ is $S = \{i, j\}$ with $\sigma_{\mathtt{T}}(S) = 10 + 15 = 25$. Adding another arbitrary node as seed node, say l, implies that $\sigma_{\mathtt{T}}(S \cup \{l\}) = 24$.

Figure 2: Example justifying non-counting of self-triggered impressions.

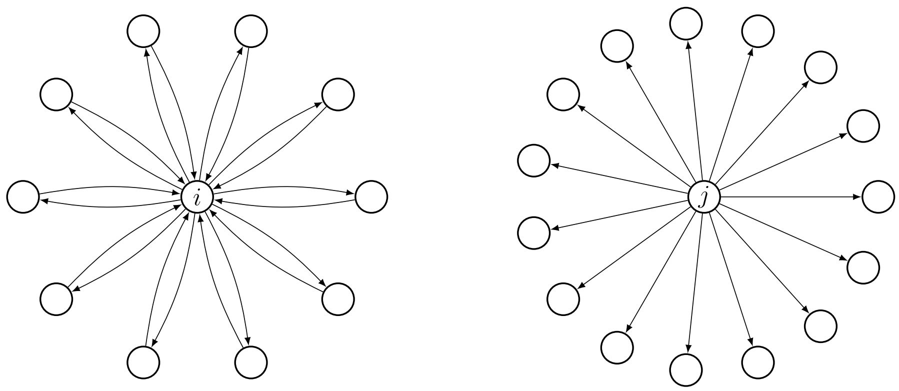

We conclude this section with Theorem 4 whose proof is given in the Appendix A for variants `O,T,R` and which is known for variant `F`, see Chen et al. [7], Kempe et al. [29].

Theorem 4. *The following results hold for each problem variant* $\mathtt{M} \in \{\mathtt{O}, \mathtt{T}, \mathtt{R}, \mathtt{F}\}$*:*

- *Problem variant* `M` *is NP-hard.*
- *The evaluation of the function* $\sigma^{\omega}_{\mathtt{M}}(S)$ *can be done in* $\mathcal{O}(|A|)$ *time.*
- *The precise evaluation of the objective function* (2) *is #P-hard.*

2.4 Extension to static competition

The proposed problem variants can be easily extended to a setting with static competition which is of particular interest if the content to be propagated relates to opinions. That is, we assume the existence of a competing entity called *leader* who already propagated a rivaling campaign from a known seed set $L \subset V$. A decision maker (called *follower*) then seeks a seed set $S \subseteq V \setminus L$ to trigger a propagation cascade as best response. We assume that the follower starts the influence propagation process after the one of the leader is over which particularly makes sense in "fast" social networks such as Twitter. Fast in this context means that the peak of impressions per second is 72 seconds after a Tweet was sent, and after 24 hours, no relevant number of impressions can be observed for 95% of all Tweets [48]. We further assume that leader seed nodes L do not forward rivaling content of the follower, thus, we can remove nodes L (and all incident arcs) from G after the leaders propagation process.

Even though the influence propagation of the leader has no substantial impact for problem variants `F`, `O`, and `T` including static competition, it has substantial implications for problem variant `R`. That is, impressions triggered by the leader have impact on a node's utility function and therefore its patronage. In such a setting a node might (i) patronize the leader, (ii) patronize the follower, or (iii) decide to stay resistant patronizing none of the latter entities. We assume that each single view of the content propagated by the leader increases a node's utility function by $\bar{a}_j + \bar{\epsilon}_j$ (similar as before). Moreover, let $\ell_j^\omega(L)$ denote the number of total impressions of the leader's content at node j in scenario $\omega \in \Omega$. Then, the *probability* that node $j \in V \setminus L$ patronizes the content triggered by the follower seed set S is given by the MNL

$$\frac{\nu_j^\omega(S)e^{\bar{b}_j}}{\ell_j^\omega(L)e^{\bar{a}_j} + \nu_j^\omega(S)e^{\bar{b}_j} + e^{\bar{r}_j}}\,.$$

Since $\ell_j^\omega(L)$ can be precomputed in this static setting, we can define $r_j^\omega(L) \coloneqq \ell_j^\omega(L)e^{\bar{a}_j} + e^{\bar{r}_j}$, and obtain the objective function of the CIMP version of variant R as

$$\sigma_{\mathtt{R}}^\omega(L,S) = \sum_{j\in V\setminus\{L\cup S\}} \frac{b_j\nu_j^\omega(S)}{b_j\nu_j^\omega(S) + r_j^\omega(L)}\,. \tag{7}$$

We refer to Appendix D for results on the latter CIMP variant. In particular we discuss the impact of considering different utilities $\bar{a}_j$ and $\bar{b}_j$ perceived from viewing the content of the leader and the follower, respectively.

3 MINLP formulation and two linearizations

In the following we propose an MINLP formulation for problem variant R and discuss adaptations of this model that allow to consider alternative objectives. Since such an MINLP model cannot be tackled by state-of-the-art solvers for mixed-integer linear and quadratic optimization, we propose two linearizations of this model to be able to deal with large-scale instances. The first linearization is based on *outer approximation* [10] and the second one on the *generalized Benders decomposition* [15].

3.1 MINLP formulation

The MINLP formulation (8) for problem variant R is based on the following sets of variables. *Forwarding variables* $f_i^\omega \in \{0,1\}$, for all $i \in V$ and $\omega \in \Omega$, indicate whether or not node i is activated in scenario ω. *Viewing variables* $v_i^\omega \in \mathbb{Z}_+$, for all $i \in V$ and $\omega \in \Omega$, represent the number of node i's impressions in scenario $\omega \in \Omega$. Finally, variables $y_i \in \{0,1\}$, for all $i \in V$, indicate whether or not node i is a seed node.

$$\max \quad \sum_{\omega\in\Omega} p^\omega \sum_{i\in V} \frac{b_i v_i^\omega}{b_i v_i^\omega + r_i} \tag{8a}$$

$$\text{s.t.} \quad \sum_{i\in V} y_i \le k \tag{8b}$$

$$\sum_{j\in\mathcal{N}_\omega^-(i)} f_j^\omega \ge v_i^\omega \qquad \forall i\in V, \forall\omega\in\Omega \tag{8c}$$

$$\sum_{j\in\mathcal{A}_\omega^-(i)} y_j \ge f_i^\omega \qquad \forall i\in V, \forall\omega\in\Omega \tag{8d}$$

$$v_i^\omega \le |\mathcal{N}_\omega^-(i)|(1-y_i) \qquad \forall i\in V, \forall\omega\in\Omega \tag{8e}$$

$$\mathbf{f}^\omega \in \{0,1\}^{|V|} \qquad \forall \omega \in \Omega \quad (8f)$$

$$\mathbf{v}^\omega \in \mathbb{Z}_+^{|V|} \qquad \forall \omega \in \Omega \quad (8g)$$

$$\mathbf{y} \in \{0,1\}^{|V|} \qquad (8h)$$

The objective function (8a) maximizes the expected patronage triggered by the seed set which is constrained by cardinality in inequality (8b). Constraints (8c) ensure that the total impressions of node i cannot exceed the number of in-neighbors activated in scenario ω. Constraints (8d) ensure that node i can only be activated in scenario ω if at least one seed node is contained in its reverse activation set $\mathcal{A}_\omega^-(i)$. Inequalities (8e) restrict the seed set from contributing to the objective function by forcing the viewing variables for all seed nodes to zero.

3.2 Choosing a different metric as objective function

The following paragraphs detail how to modify formulation (8) for alternative objectives.

Maximizing the number of total impressions (`T`). The only change required in (8) to maximize the expected number of total impressions is to replace objective function (8a) by

$$\max \sum_{\omega \in \Omega} p^\omega \sum_{i \in V} v_i^\omega \,. \qquad (9)$$

Maximizing the organic reach (`O`). To maximize the expected organic reach, in addition to the objective function defined in (9), the term $|\mathcal{N}_\omega^-(i)|$ in (8e) is replaced by one. Then, variables v_i^ω, for all $i \in V$ and $\omega \in \Omega$, are bounded from above by one and indicate whether or not node i views a content at least once in scenario ω.

Maximizing the number of active nodes (`F`). The classical objective of IMPs (in the spirit of Kempe et al. 29) is to maximize the expected number of active nodes. As passive viewing events do not exist in such variants, viewing arcs $A^\omega \setminus \underline{A}^\omega$ are removed from scenario graphs G^ω, for all $\omega \in \Omega$. Thus, we can also remove viewing variables $\mathbf{v} \in \mathbb{R}_+^{|V| \times |\Omega|}$ and all constraints where they appear, i.e., (8c) and (8e). Finally, the objective function (8a) is replaced by

$$\max \sum_{\omega \in \Omega} p^\omega \sum_{i \in V} f_i^\omega \,, \qquad (10)$$

so that we obtain exactly the same formulation as used in Güney et al. [20].

3.3 Linearization based on outer approximation

Outer approximation (OA) introduced by Duran and Grossmann [10] and later improved by Fletcher and Leyffer [14] is one option for linearizing formulation (8). We focus on the multi-cut variant of the OA (see, e.g., Mai and Lodi 41), by exploiting the separability of the objective function. We only discuss the model for problem variant `R`, given that the OA approach is redundant for the remaining ones, as their objective functions are already linear.

Let $u^\omega \in \mathbb{R}_+$, for all $\omega \in \Omega$, denote the objective function contribution of scenario $\omega \in \Omega$ and let $g^\omega(\mathbf{v}) = \sum_{i\in V} \frac{b_i v_i^\omega}{b_i v_i^\omega + r_i}$. Let further $P_{\mathbf{v}} \coloneqq \{\mathbf{v} \in \mathbb{Z}_+^{|V|} : (8b) - (8h)\}$ denote the set of all feasible integer viewing variables. Then, after applying OA to (8) we obtain reformulation (11).

$$\text{(OA)} \quad \max \quad \sum_{\omega\in\Omega} p^\omega u^\omega \tag{11a}$$

$$\text{s.t.} \quad u^\omega \leq \sum_{i\in V} \frac{b_i \bar{v}_i^\omega}{b_i \bar{v}_i^\omega + r_i} + \sum_{i\in V} \bar{m}_i^\omega (v_i^\omega - \bar{v}_i^\omega) \qquad \forall \bar{\mathbf{v}} \in P_{\mathbf{v}},\ \forall \omega \in \Omega \tag{11b}$$

Here $\bar{m}_i^\omega$ denotes the the first-order partial derivative of the concave function $g^\omega(\mathbf{v})$ with respect to viewing variables $\mathbf{v}^\omega$, i.e.,

$$\bar{m}_i^\omega = \frac{\partial g^\omega(\bar{\mathbf{v}})}{\partial v_i^\omega} = \frac{b_i r_i}{(b_i \bar{v}_i^\omega + r_i)^2}\,. \tag{12}$$

Formulation (11) contains a finite but exponential number of constraints (11b), due to the fact that variables $\mathbf{v}$ take on integer values, and since there is only a finite number of points (namely, $|P_{\mathbf{v}}|$) in which the function $g^\omega(\mathbf{v})$ has to be approximated with its tangential hyperplane. Such models are typically solved using branch-and-cut. Unfortunately, the number of variables $\mathcal{O}(|V||\Omega|)$ makes this model prohibitive for solving instances of realistic size. We therefore proceed by investigating a computationally more tractable approach (generalized Benders decomposition), in which the number of variables is reduced to $\mathcal{O}(|V| + |\Omega|)$.

3.4 Linearization based on generalized Benders decomposition

In contrast to OA in which the problem is modeled in the full variable space, the *generalized Benders decomposition* [15] projects out forwarding and viewing variables and exploits dual information to generate linear approximations of the objective function. To be able to proceed with this approach, Lemma 5 provides a crucial result which states that integrality constraints for the forwarding and viewing variables ((8f)-(8g)) can be relaxed.

Lemma 5. *Given an optimal solution $\mathbf{y}^* \in P_{\mathbf{y}} \coloneqq \{\mathbf{y} \in \{0,1\}^{|V|} : \sum_{i\in V} y_i \leq k\}$, there exist optimal integral values for relaxed forwarding and viewing variables $\mathbf{f}^* \in [0,1]^{|V|\times|\Omega|}$ and $\mathbf{v}^* \in \mathbb{R}_+^{|V|\times|\Omega|}$ in (8) implied by $\mathbf{y}^*$.*

The reformulation is now obtained from projecting out continuous variables $\mathbf{f}$ and $\mathbf{v}$ (cf., Lemma 5) from the master problem into $|\Omega|$ linearly constrained subproblems. The latter subproblems can be solved in polynomial time (cf., Theorem 7). Reformulation (13) for variant `R` is stated in Theorem 6 whose proof is given in Appendix A. For the remaining problem variants, namely `T`, `O`, `F`, the (generalized) Benders decomposition approach can also be applied, yielding different families of cuts, which are summarized in Corollaries 1-3.

Let $P_{\mathbf{y}} \coloneqq \{\mathbf{y} \in \{0,1\}^{|V|} : \sum_{i\in V} y_i \leq k\}$ and assume that a bar $\bar{\cdot}$ over sets and variables indicates their values implied by a candidate solution $\bar{\mathbf{y}} \in P_{\mathbf{y}}$. For instance, $\bar{S} = \{i \in V : \bar{y}_i = 1\}$ at point $\bar{\mathbf{y}} \in P_{\mathbf{y}}$, while $\bar{\mathbf{f}}$ and $\bar{\mathbf{v}}$ denote the values of the forwarding and viewing variables associated with $\bar{\mathbf{y}}$, respectively. Set $\bar{V}^\omega \coloneqq \{i \in V : \nu_i^\omega(\bar{S}) = |\mathcal{N}_\omega^-(i)|\} \cup \{\bar{S}\}$ further denotes the set of *saturated nodes* who either attained their maximum number of total impressions in scenario ω or are seed nodes (who are saturated with zero impressions by definition).

Theorem 6. *Formulation* (13) *is a reformulation of* (8) *in the* $(\mathbf{u}, \mathbf{y})$*-space for problem variant* `R`*.*

$$
\begin{aligned}
(\mathtt{GB}) \quad & \max \quad \sum_{\omega \in \Omega} p^\omega u^\omega && && \text{(13a)} \\
& s.t. \quad u^\omega \leq \sigma^\omega_{\mathtt{R}}(\bar{S}) - \sum_{i \in \bar{S}} \bar{\rho}^\omega_i (1 - y_i) + \sum_{i \notin \bar{S}} \bar{\rho}^\omega_i y_i && \forall \bar{S} \subseteq V, \forall \omega \in \Omega && \text{(13b)} \\
& \qquad \mathbf{y} \in P_{\mathbf{y}} && && \text{(13c)}
\end{aligned}
$$

where

$$
\bar{\rho}^\omega_i = \begin{cases} -|\mathcal{N}^-_\omega(i)| \bar{m}^\omega_i & \text{if } i \in \bar{S} \\ \sum_{j \in \mathcal{A}_\omega(i) \setminus \mathcal{A}_\omega(\bar{S})} \sum_{k \in \mathcal{N}_\omega(j)} \bar{m}^\omega_k & \text{if } i \in V \setminus \bar{V}^\omega \\ \sum_{j \in \mathcal{A}_\omega(i) \setminus \mathcal{A}_\omega(\bar{S})} \sum_{k \in \mathcal{N}_\omega(j)} \bar{m}^\omega_k - |\mathcal{N}^-_\omega(i)| \bar{m}^\omega_i & \text{if } i \in \bar{V}^\omega \setminus \bar{S} \end{cases} \quad \forall \omega \in \Omega, \quad \forall i \in V. \tag{14}
$$

Here $\bar{\boldsymbol{\rho}}^\omega$ denotes the supergradient of the objective function of the Benders subproblem in scenario $\omega \in \Omega$ at point $\bar{\mathbf{y}} \in P_{\mathbf{y}}$ and $\bar{m}^\omega_i$ is defined as in (12). Constraints (13b) are (exponentially many) generalized Benders optimality cuts. Note that no feasibility cuts are needed since every $\mathbf{y} \in P_{\mathbf{y}}$ is feasible.

The result of Theorem 6 can be easily adapted to the other problem variants outlined in Section 3.2.

Corollary 1. *For problem variant* `T`*, formulation* (13) *is a reformulation of* (8) *in the* $(\mathbf{u}, \mathbf{y})$*-space after replacing* $\sigma^\omega_{\mathtt{R}}(\bar{S})$ *with* $\sigma^\omega_{\mathtt{T}}(\bar{S})$ *in* (13b) *and setting* $\bar{m}^\omega_i = 1$*, for all* $i \in V$*,* $\omega \in \Omega$*, in* (14)*.*

Corollary 2. *For problem variant* `O`*, formulation* (13) *is a reformulation of* (8) *in the* $(\mathbf{u}, \mathbf{y})$*-space after replacing* $\sigma^\omega_{\mathtt{R}}(\bar{S})$ *with* $\sigma^\omega_{\mathtt{O}}(\bar{S})$ *in* (13b) *and setting* $\bar{m}^\omega_i = 1$*, for all* $i \in V$*,* $\omega \in \Omega$*, and* $|\mathcal{N}^-_\omega(i)| = 1$*, for all* $i \in V$*,* $\omega \in \Omega$*, in* (14)*.*

Corollary 3. *For problem variant* `F`*, formulation* (13) *is a reformulation of* (8) *in the* $(\mathbf{u}, \mathbf{y})$*-space after replacing* $\sigma^\omega_{\mathtt{R}}(\bar{S})$ *with* $\sigma^\omega_{\mathtt{F}}(\bar{S})$ *in* (13b) *and replacing* (14) *with*

$$
\bar{\rho}^\omega_i = \begin{cases} 0 & \text{if } i \in \bar{S} \\ |\mathcal{A}_\omega(i) \setminus \mathcal{A}_\omega(\bar{S})| & \text{otherwise,} \end{cases} \quad \forall \omega \in \Omega, \quad \forall i \in V\,.
$$

We refer to Appendix A for details and point out that the result stated in Corollary 3 corresponds to the Benders reformulation for problem variant `F` studied by Güney et al. [20]. It is known that OA cuts dominate the ones from generalized Benders decomposition [10] and that the latter cuts correspond to aggregated OA cuts [49]. While OA algorithms need fewer iterations than generalized Benders decomposition algorithms to converge to an optimal solution, this comes at the cost of having (significantly) more variables in the master problem. Duran and Grossmann [10] state that OA may therefore have benefits if the non-linear subproblems are computationally costly. As shown in Theorem 7 this is, however, not the case.

Theorem 7. *For a given* $\omega \in \Omega$*, the separation of generalized Benders cuts* (13b) *can be done in* $\mathcal{O}(|V|^2)$ *time for all problem variants* `F`*,* `O`*,* `T`*, and* `R`*.*

4 Heuristics

In this section, we exploit the submodularity properties (cf., Theorems 1-3) to show the existence of worst-case guarantees when solving our IMP variants with marginal gain heuristics. Moreover, we discuss frequently used (topology-based) heuristics to which we compare our approach in Section 7.4.

4.1 Marginal gain heuristics for problem variants `O`, `T`, `R`

The greedy heuristic of Nemhauser et al. [44] with a worst-case approximation ratio of $1 - 1/e$ provides a simple and effective way to obtain high-quality solutions for maximizing *non-decreasing* submodular functions subject to a cardinality constraint. While this result is valid for problem variant `F` introduced by Kempe et al. [29] and Bharathi et al. [4], it does not extend to the other variants studied in this paper (since the monotonicity property is violated). The greedy heuristic of Nemhauser et al. [44], referred to as the *marginal gain* (`MG`) heuristic starts with an empty seed set $\tilde{S}$ and iteratively inserts a node i with maximum positive marginal gain $\sigma_{\mathtt{M}}(\tilde{S} \cup \{i\}) - \sigma_{\mathtt{M}}(\tilde{S})$. In our case, the calculation of this marginal gain is based on a propagation applied to scenario graphs for each scenario $\omega \in \Omega$. The algorithm stops after at most k iterations (given that σ is not monotone, the algorithm may stop earlier if there are no more nodes with positive marginal gain). In the following, we provide the quantitative assessment of the solutions obtained through this greedy procedure.

Theorem 8. *For problem variants $\mathtt{M} \in \{\mathtt{O}, \mathtt{T}, \mathtt{R}\}$, the `MG` heuristic finds a seed set $\tilde{S} \subseteq V$ such that*

$$\sigma_{\mathtt{M}}(\tilde{S}) \geq (1 - 1/e)\sigma_{\mathtt{M}}(S^*) - k\alpha^k\theta$$

where $S^* \subseteq V$ is an optimal solution, $\alpha = (k-1)/k$ and $\theta = 1$ for the variants `R`,`O`, and $\theta = \max_{i \in V} |\mathcal{N}^-(i)|$ for the variant `T`.

Remark 2. Without restricting seed nodes to contribute to the objective function in variant `O`, we would obtain the well-known $1 - 1/e$ approximation ratio instead of the result stated in Theorem 8.

The fact that the precise evaluation of function $\sigma_{\mathtt{M}}(S)$ is #P-hard (cf., Theorem 4) due to the exponential number of scenarios Ω impedes the efficient solution of all problem variants. A common remedy is to approximate $\sigma_{\mathtt{M}}(S)$ by considering only a subset of scenarios $\Omega' \subset \Omega$ (of polynomial size). Kempe et al. [30] showed that such an approximation can be used to obtain an $(1 - 1/e - \epsilon)$-approximation for variant `F` and arbitrary $\epsilon > 0$. Their result allows to adapt the approximation factor in Theorem 8 and therefore implies **??** 4**??** 5.

Corollary 4. *There exist polynomial-time algorithms for problem variants $\mathtt{M} \in \{\mathtt{O}, \mathtt{R}\}$ that find a seed set $\tilde{S} \subseteq V$ such that*

$$\sigma_{\mathtt{M}}(\tilde{S}) \geq (1 - 1/e - \varepsilon)\sigma_{\mathtt{M}}(S^*) - k/e$$

where $S^* \subseteq V$ is an optimal solution.

Corollary 5. *There exists a polynomial-time algorithm for problem variant `T` that finds a seed set $\tilde{S} \subseteq V$ such that*

$$\sigma_{\mathtt{T}}(\tilde{S}) \geq (1 - 1/e - \varepsilon)\sigma_{\mathtt{T}}(S^*) - M \cdot k$$

where $S^* \subseteq V$ is an optimal solution and $M = \frac{1}{e}\max_{i \in V} |\mathcal{N}^-(i)|$.

To summarize, in this section we showed that for solving problem variants O,T,R, high-quality solutions with worst-case bounds can be obtained by applying the greedy heuristic MG. While we were not able to derive a constant approximation ratio, the solutions found by the heuristic can still be relevant for practical applications, in particular when the size of the seed set k is bounded by a constant and when the right-most terms of the inequalities given in ?? 4?? 5 are negligible compared to the optimal solution value. Although the quality of solutions found by MG is typically much better than suggested by the worst-case bounds, one can easily derive instances for which the worst-case bounds are tight (see, e.g., Coniglio et al. [8] or Hochbaum and Pathria [23] for similar examples). The latter downside can be overcome by using the *exact algorithms* based on the branch-and-cut procedures introduced in Section 3. The worst-case complexity of these algorithms is exponential, however, the major advantage compared to (greedy) heuristics is in the possibility to stop the computations after a given (time-)limit and obtain provable dual bounds that allow to better estimate the quality of the obtained solution. Another important advantage of MINLP-based models is the fact that their cardinality constraint (choose at most k nodes as the seed set) can be easily generalized into, e.g., a knapsack constraint, matroid-based constraints, or even conflict or connectivity constraints. These changes are trivial to integrate into MINLP models, but require a complete restructuring of underlying approximation heuristics and the theoretical approximation guarantees (or worst-case bounds) may be lost.

4.2 Topology-based heuristics

We now outline six topology-based heuristics whose performance will be empirically compared to the MG heuristic (cf., Section 4.1) and the exact methods (cf., Section 3.4).

All considered topology-based heuristics use a given criterion to first compute influence values $d_i \geq 0$, for all $i \in V$; see Table 1 for a summary. After sorting all nodes in non-increasing order with respect to this criterion, the first (best) k nodes are chosen as seed set S. The following concepts and notations are used in Table 1:

- The *outdegree centrality* heuristic (DC) uses the fact that nodes with a large outdegree in instance graph G are likely to activate more users than nodes with a low outdegree.
- The *expected outdegree* heuristic (EC) works similar, however, uses the expected node outdegree in scenario graph G^ω, $\omega \in \Omega$, as ranking criterion.
- The *betweenness centrality* heuristic (BC) uses the total numbers of shortest paths c_{st} from s to t and the number $c_{st}(i)$ of these shortest paths containing node i, $i \notin \{s, t\}$.
- For the *reverse PageRank* heuristic (PR), $\lambda \in [0, 1]$ is a damping factor which we set to $\lambda = 0.85$ in our computations like it was first used by Google [45]. This recursive algorithm converges fast and stops if the error between two iterations t and $t+1$ measured in the L_1-norm $\|\mathbf{d}_t - \mathbf{d}_{t+1}\|_1$ is below some threshold (we set 10^{-6}). PageRank proposed by Page et al. [47] estimates the importance of websites. Here, websites are considered as important if other important websites link to them. For identifying influential nodes in social networks the procedure is reversed [24]. Nodes are considered to be influential if they are followed by other influential ones.
- The *TunkRank* heuristic (TR) is a PageRank analogue to Twitter [63] in which M denotes the number of followers of node i. We set $M = |\mathcal{N}^-_\omega(i)|$ in our experiments and use the same

Table 1: Ranking criteria d_i for nodes $i \in V \setminus L$ of the topology-based heuristics.

Ranking criterion (`heuristic`)	d_i
Outdegree centrality (`DC`)	$\lvert\mathcal{N}(i)\rvert$
Expected outdegree centrality (`EC`)	$\mathbb{E}[\lvert\mathcal{N}_\omega(i)\rvert] = \sum_{\omega\in\Omega'} p^\omega \sum_{j\in\mathcal{N}_\omega(i)} p^{\mathrm{f}}_{ij}$
Betweenness centrality (`BC`)	$\sum_{s\neq t\in V, i\in V\setminus\{s,t\}} \frac{c_{st}(i)}{c_{st}}$
Reverse PageRank (`PR`)	$\frac{1-\lambda}{\lvert V\rvert} + \lambda \sum_{j\in\mathcal{N}(i)} \frac{d_j}{\lvert\mathcal{N}^-(i)\rvert}$
TunkRank (`TR`)	$\sum_{j\in\mathcal{N}(i)} \frac{1+p^{\mathrm{f}}_{ij} d_j}{\lvert M\rvert}$
Retweet, answers, mentions (`RM`)	$\frac{o_i+w_i+z_i}{\sum_{i\in V} o_i+w_i+z_i}$

stopping threshold as for `PR`.

- Leavitt et al. [36] proposed the heuristic based on *retweets, answers and mentions* (`RM`). Here, o_i denotes how often node i is retweeted, and w_i and z_i denote how often node i is replied to and how often node i is mentioned by other nodes, respectively (see Section 5 for a description how we obtained these values).

5 Benchmark instances

Real-world benchmark instances were created by querying information of users, tweets and their relation to each other using Twitter's developer interface in its freely available standard version 1.1 [54]. Instance graphs were built by first choosing a hashtag (e.g., #giftideas) and then searching for tweets (of the last seven days) that include this hashtag. The authors of these tweets defined the initial node set of an instance. Next, all tweets of this initial node set from the year 2020 were analyzed in detail. Only the latest 3 200 tweets were considered for users whose number of tweets from 2020 exceeded 3 200 (which is a limitation of the free developer interface of Twitter in the used version 1.1). Whenever one of these tweets included the chosen hashtag and retweets, quotes, replies to, or mentions users not yet included in the instance, these users were added and their tweets were analyzed in the same way. The procedure was stopped when no more new users were added. We generated eight instances using the hashtags #austria, #giftideas, #greenenergy, #naturelovers, #organicfood, #orms (operations research and management science), #skateboarding, and #travelling. These hashtags were chosen as examples for content used to promote products, events, cultural activities, or accommodation offers. The forwarding probability p^{f}_{ij} of each arc $(i,j) \in A$ was computed as

$$p^{\mathrm{f}}_{ij} = \frac{retweets_{ji} + answers_{ji}}{|T_j| + |R_j| + |A_j|}$$

where $retweets_{ji}$ and $answers_{ji}$ correspond to how often user j retweeted something from and answered to user i, respectively. Moreover, T_j, R_j, and A_j are the sets of original tweets, retweets and answers of user j, respectively. Thus, fractions (or probabilities) of actions from user j that refer to user i were computed. For instance, if user j had an output of 100 tweets whereby one of them was a retweet of user i, the probability that the output from j contains a message forwarded from i is $^1/_{100}$. Note that summing up the terms in the numerator of the expression above, yields the corresponding values used in heuristic `RM`, e.g., $o_i = \sum_{j\in\mathcal{N}(i)} retweets_{ji}$.

Table 2: Real-world social network instances.

Instance graph name	$\lvert V\rvert$	$\lvert A\rvert$	$\overline{\delta}(i)$	$\mathbb{E}[\delta(i)]$	Description (retrieval date)
`tw-austria`	4 753	57 353	12.1	0.15	#austria (2020/08/14)
`tw-giftideas`	4 541	336 855	148.3	0.46	#giftideas (2020/08/10)
`tw-greenenergy`	3 040	26 199	17.2	0.13	#greenenergy (2020/08/11)
`tw-naturelovers`	14 108	664 713	47,1	0.24	#naturelovers (2020/08/09)
`tw-organicfood`	390	923	4.7	0.11	#organicfood (2020/08/13)
`tw-orms`	546	3 659	13.4	0.29	#orms (2020/08/07)
`tw-skateboarding`	2 700	17 302	12.8	0.13	#skateboarding (2020/08/10)
`tw-travelling`	1 661	6 877	8.3	0.10	#travelling (2020/08/08)
`msg-college`	1 899	20 296	21.4	0.04	Leskovec and Krevl [38]
`msg-email-eu`	986	24 929	50.6	0.11	Leskovec and Krevl [38]
`soc-advogato`	5 167	47 322	18.3	0.04	Rossi and Ahmed [55]
`soc-anybeat`	12 645	67 053	10.6	0.02	Rossi and Ahmed [55]

Note. We report numbers of nodes $|V|$, numbers of directed arcs $|A|$, average node degrees $\overline{\delta}(i)$, and expected node degrees $\mathbb{E}[\delta(i)] = \frac{1}{|\Omega'|}\sum_{\omega\in\Omega'}\left(\sum_{j\in\mathcal{N}^-_\omega(i)} p^{\mathrm{f}}_{ji} + \sum_{j\in\mathcal{N}_\omega(i)} p^{\mathrm{f}}_{ij}\right)$ where $\Omega' \subset \Omega$ (cf., Section 6.1).

The approximately 10^6 observations (combined over all instances) result in an empirical distribution of the forwarding probability with the following characteristics: average = 0.04%, minimum = 0.03%, Q_1 = 0.03%, Q_2 = 0.09%, Q_3 = 0.3%, maximum = 100%, where Q_{x} denotes the x^{th} quartile of the distribution. The latter distribution was used to extend benchmark instances from the literature (Leskovec and Krevl 38, Rossi and Ahmed 55). Missing probabilities p^{f}_{ij}, $(i,j)\in A$, were estimated by drawing random samples from the aforementioned empirical distribution. Some of these graphs also contained parallel arcs that reflect messages sent at different points in time. Notice that we collapsed such parallel arcs to only one arc, because we are mainly interested in node relationships.

An overview over all used instances is given in Table 2. Visualizations of the distribution of (expected) in- and outdegrees of these instances are provided in the Appendix E.

6 Algorithmic framework

This section details our algorithmic framework and parameters used in our computational study.

6.1 Sample average approximation

Considering all scenarios $|\Omega| = 3^{|A|}$ is computationally intractable even for small instances. We therefore embed our branch-and-cut framework in a sample average approximation (SAA) scheme [32]. In each SAA iteration, a much smaller set of independently drawn and identically distributed scenarios $\Omega' \subset \Omega$ is considered. The solution of each SAA iteration is subsequently evaluated on a much larger set of scenarios $|\Omega''| \gg |\Omega'|$ and the solution which performs best on set Ω'' is chosen as the best approximation of the optimal solution. Consequently, we adapt the objective function (8a) to

$$\hat{\sigma}_{\mathrm{R},\Omega'}(\hat{S}) = \frac{1}{|\Omega'|}\sum_{i\in V}\frac{b_i v_i^\omega}{b_i v_i^\omega + r_i}$$

where a hat $\hat{\cdot}$ indicates an estimator. Notice that a seed set $\hat{S}$ is an estimator too (due to the SAA approach). The objective functions for all other problem variants are adapted analogously. For the sake of brevity we will neglect the subscript Ω'' for indicating objective function values evaluated on set Ω'' and instead denote such estimated values by $\hat{\sigma}_{\mathtt{M}}(\hat{S})$.

As we cannot guarantee to solve each SAA iteration to optimality, we use the inexact SAA [3] to estimate the approximation gap Δ as

$$\Delta = \frac{\mathrm{UB}_{\Omega'}(\hat{S}) - \mathrm{LB}_{\Omega''}(\hat{S})}{\mathrm{UB}_{\Omega'}(\hat{S})}\,.$$

Here, $\mathrm{UB}_{\Omega'}(\hat{S})$ and $\mathrm{LB}_{\Omega''}(\hat{S})$ are the approximated $1-\alpha$ confidence upper and lower bounds, respectively; see Bardossy and Raghavan [3] for further details.

6.2 Scenario graphs and (reverse) activation sets

Generation of scenario graphs. We use a sampling procedure in which a number $\xi_{ij}^{\omega} \in [0,1]$ is drawn independently and uniformly at random for each scenario $\omega \in \Omega'$ and every arc $(i,j) \in A$. If $\xi_{ij}^{\omega} \le p_{ij}^{\mathrm{f}}$ node j can be activated by i in scenario ω and, thus, $(i,j) \in \underline{A}^{\omega}$. Node j, however, only views content received from node i in scenario ω if $p_{ij}^{\mathrm{f}} < \xi_{ij}^{\omega} \le p_{ij}^{\mathrm{v}}$, i.e., $(i,j) \in A^{\omega} \setminus \underline{A}^{\omega}$. Influence attempts fail in scenario ω if $p_{ij}^{\mathrm{v}} < \xi_{ij}^{\omega}$ in which case $(i,j) \notin A^{\omega}$.

Computation of (reverse) activation sets. Reverse activation sets are computed by a reverse BFS on subgraph $(V, \underline{A}^{\omega})$ from each node $i \in V$ and for each scenario $\omega \in \Omega'$. The propagation stops when a node j for which $\mathcal{A}_{\omega}^{-}(j)$ is already known is encountered. In the latter case, all nodes from $\mathcal{A}_{\omega}^{-}(j)$ are added to $\mathcal{A}_{\omega}^{-}(i)$, because then $\mathcal{A}_{\omega}^{-}(j) \subset \mathcal{A}_{\omega}^{-}(i)$. A forward BFS is used to compute sets $\mathcal{A}_{\omega}(i)$, for all $i \in V$, $\omega \in \Omega'$.

6.3 Preprocessing singletons

A *singleton* node $i \in V$ in scenario ω has an objective function contribution of zero in that scenario. Thus, corresponding viewing variables v_i^{ω} can be forced to zero and the corresponding constraints (8c)-(8e) can be removed. Respective supergradient coordinates $\bar{\rho}_i^{\omega} = 0$, $\bar{\mathbf{y}} \in P_{\mathbf{y}}$ are enforced in reformulation (13). Thus, the number of nodes considered in the separation of the generalized Benders cuts can be reduced by this preprocessing procedure.

6.4 Separation of generalized Benders cuts

To avoid that the initial LP relaxation is unbounded, we initially include Benders cuts

$$u^{\omega} \le \sum_{i \in V} \bar{\rho}_i^{\omega} y_i \qquad\qquad \forall \omega \in \Omega',$$

that correspond to (13b) for $\bar{\mathbf{y}} = \mathbf{0}$ in (13). Further Benders cuts are generated on-the-fly in an LP-based branch-and-cut fashion for integer as well as fractional solutions $\bar{\mathbf{y}} \in P'_{\mathbf{y}} := \{[0,1]^{|V|} : \sum_{i \in V} y_i \le k\}$. Theorem 7 shows that these cuts can be separated in $\mathcal{O}(|V|^2)$. The separation algorithm (that we use for fractional solutions) follows the relations obtained in the proofs of Theorem 6 and Corollaries 1-3 given in Appendix A. A simpler method is used for integer solutions

$\bar{\mathbf{y}} \in P_{\mathbf{y}}$; see Algorithm 1 in Appendix B. Here, we propagate directly from $\bar{S} = \{i \in V : \bar{y}_i = 1\}$ along $\mathcal{A}_\omega(\bar{S})$ while considering all out-neighbors $\mathcal{R}_\omega(\bar{S})$ to obtain the current value of $\sigma^\omega_{\mathtt{M}}(\bar{S})$ for each scenario $\omega \in \Omega'$.

7 Computational results

In this section, we report the results of our computational study and discuss their managerial implications. We first detail used parameter settings in Section 7.1 before identifying an appropriate number of scenarios $|\Omega'|$ considered in the computations in Section 7.2. In Section 7.3 we compare the performance of the generalized Benders decomposition and the outer approximation approach. Section 7.4 evaluates the solution quality obtained by the heuristics discussed in Section 4.2 compared to those obtained by the generalized Benders decomposition algorithm based on model (13). In Section 7.5, we focus on the impact of different solutions obtained from problem variants `F`, `O`, `T`, and `R`, by cross-validating them on all (other) metrics. Finally, we analyze the lengths of propagation cascades in Section 7.6.

All algorithms were implemented in *julia* 1.1.0 and each experiment was performed on a single core of an Intel Xeon E5-2670v2 machine with 2.5 GHz and 32 GB RAM. IBM CPLEX 12.9 (with default settings) was used as ILP solver, and a time limit of two hours per SAA iteration was set. The program code, the instance graphs, and results are provided in the accompanying online repository [26].

7.1 Parameter setting

One limitation of the free version of the Twitter developer interface (version 1.1) is that the collection of data that allow the estimation of resistance values and viewing probabilities is prohibited, so that we set viewing probabilities to $p^{\mathrm{v}}_{ij} = 5\%$, for all $(i,j) \in A$. The latter value is a compromise between Stone [59] who states that the organic reach on Facebook is 6.4% and Virgillito [64] who states that the organic reach on Twitter is around 3.6%. To facilitate an analysis of the impact of resistant nodes, we assume that a node is resistant if its patronizing probability (5) does not exceed a given *resistance hurdle* $h \in (0,1]$ which we set to $h = 0.1$. That is, a node $i \in V$ is resistant in our setting if $\max_{\omega \in \Omega} \frac{b_i|\mathcal{N}^-_\omega(i)|}{b_i|\mathcal{N}^-_\omega(i)|+r_i} \leq \frac{b_i|\mathcal{N}^-(i)|}{b_i|\mathcal{N}^-(i)|+r_i} \leq h$. Note that the latter inequality is tight if $r_i = \max\{1, \frac{1-b_ih}{h}|\mathcal{N}^-(i)|\}$ and $|\mathcal{N}^-(i)| > 0$, thus, we use the latter equation to compute the values r_i for resistant nodes $i \in V$. The resistance values of all other nodes are randomly chosen integers from the interval $[1, \frac{1-b_ih}{h}|\mathcal{N}^-(i)|]$ if $|\mathcal{N}^-(i)| > 0$ whereas $r_i = 1$ is used if $\mathcal{N}^-(i) = \emptyset$. Note that this approach avoids too large resistance values which may cause numerical instabilities. For the computational experiments whose results are reported in Sections 7.2-7.4 we choose resistant nodes randomly. More fine-grained selection criteria are used and reported in Sections 7.5 and 7.6. The utilities b_i perceived from viewing content are set to one for all $i \in V$. Generalized Benders cuts at fractional points are only added if they are violated by at least 0.1%. In total, ten SAA iterations are performed for each computational experiment, and the solution which performs best on $|\Omega''| = 100\,000$ independently generated scenarios is chosen.

7.2 Appropriate number of scenarios

To identify an appropriate number of scenarios $|\Omega'|$ we analyze solutions obtained with our generalized Benders decomposition algorithm for $|S| \in \{5, 10, 15\}$, and $|\Omega'| \in \{100, 250, 500, 750\}$. The choice of $|\Omega'|$ is then based on the achieved relative approximation gaps (cf., Section 6.1) and the average in-sample and out-of-sample stabilities [28] shown in Figure 3. The latter correspond to the average relative differences between the solutions of each SAA iteration evaluated on sets Ω' and Ω'', respectively.

The results shown in Figure 3 confirm that approximation gaps Δ, in-sample and out-of-sample stabilities decrease with increasing number of scenarios $|\Omega'|$. Comparing the solutions per instance and parameter configuration surprisingly reveals, however, that the seed sets identified for different numbers of scenarios are always identical when fixing all other parameter values. Taking into account the CPU-times required per SAA iteration (see Figure 8 in Appendix C), we conclude that $|\Omega'| = 100$ seems the best choice for our remaining experiments even though obtained approximation gaps are slightly larger.

Figure 3: Approximation gaps Δ, in-sample stabilities, and out-of-sample stabilities in percent.

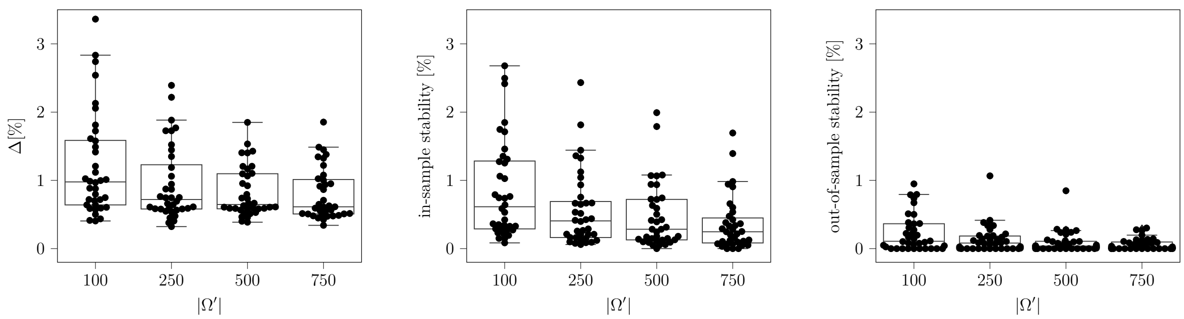

7.3 Empirical comparison with outer approximation

For problem variant `R`, we compare the performance of generalized Benders decomposition (`GB`) and outer approximation (`OA`). Both methods are implemented as branch-and-cut algorithms in which cutting planes are separated at each node of the branching tree.

The performance profiles in Figure 4 summarize the results obtained over all used instances and the aforementioned parameter settings. We observe that `GB` significantly outperforms `OA`. For more than 30% of the instances, `OA` reaches the time limit whereas most of them can be solved by `GB`. This can be explained by the significantly larger number of variables required for the reformulation based on outer approximation. Even for 100 scenarios, this number grows rapidly, and prohibits an efficient exploration of the search space. Therefore, based on these results, we desist from reporting further results obtained from the `OA` algorithm.

7.4 Empirical quality of heuristic solutions

This section sheds light into the question whether or not `GB` has significant benefits over heuristic methods in terms of solution quality (in addition to providing either a proof of optimality or a dual bound).

Figure 4: Performance profiles of generalized Benders decomposition (GB) and outer approximation (OA).

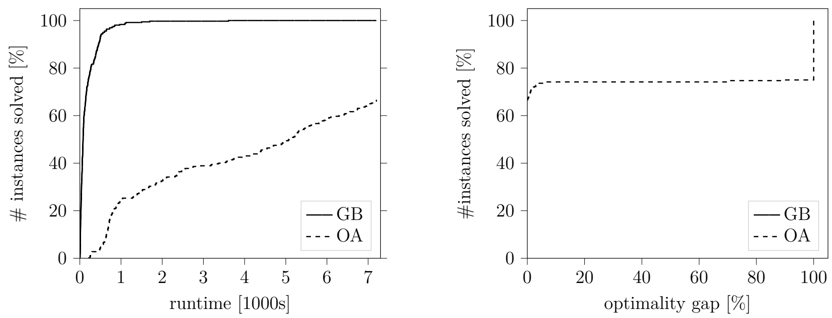

Note. Optimality gaps are computed by (UB − OV)/UB where UB denotes the best known upper bound and OV denotes the objective value of the corresponding SAA iteration. Note that $|\Omega'| = 100$.

Figure 5: Heuristic solution qualities in percent.

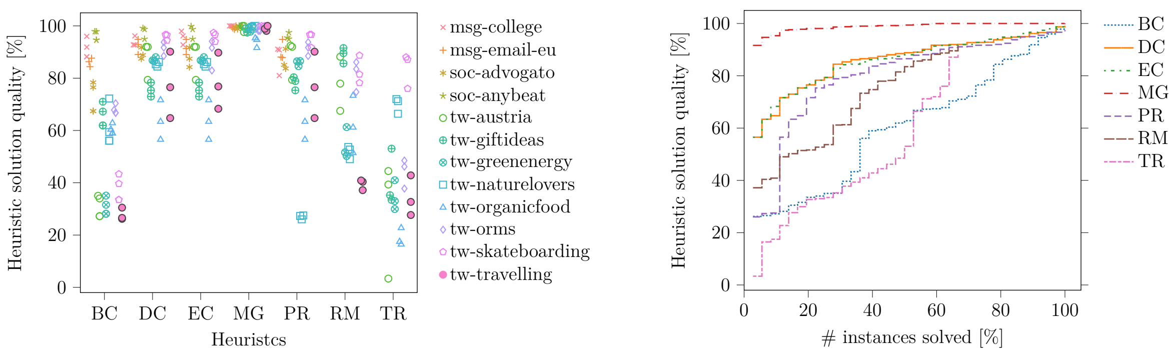

Figure 5 shows objective values obtained from all heuristics described in Section 4.2 relative to those of the GB. Let $\hat{\sigma}_{\mathtt{R}}(\hat{S}^*)$ denote the objective value of the GB, and $\hat{\sigma}_{\mathtt{R}}(\hat{S}^*_{\mathtt{H}})$ denotes the one derived from evaluating seed set $\hat{S}^*_{\mathtt{H}}$ obtained from heuristic $\mathtt{H} \in \{\mathtt{BC}, \mathtt{DC}, \mathtt{EC}, \mathtt{MG}, \mathtt{PR}, \mathtt{RM}, \mathtt{TR}\}$ on metric R. Then, the relative heuristic solution qualities are computed as

$$\frac{\hat{\sigma}_{\mathtt{R}}(\hat{S}^*_{\mathtt{H}})}{\hat{\sigma}_{\mathtt{R}}(\hat{S}^*)}.$$

We observe that using one of the considered heuristics instead of an exact method such as GB can lead to substantial losses in terms of objective values (up to 80% for BC and PR, and up to 50% for DC and EC). This observation holds for all heuristics but MG, where the losses are at most 10%. MG delivers good results but requires a substantial amount of time. We refer to Appendix C for detailed results including runtimes. We remark, however, at this point that there is no clear trend whether MG or GB (which, contrary to MG, also delivers a proof of optimality) is faster. It is surprising to see that the runtimes of an exact method with an exponential worst-case runtime, when evaluated on realistic instances, are often similar and frequently even substantially smaller than those of a heuristic whose runtime is polynomial.

7.5 Impact of passive viewing (and resistant nodes) in influence maximization

We now analyze the impact of considering passive social viewing events (and resistant nodes) in IMPs. The focus is on showing how much improvement in terms of organic reach ($\mathtt{O}$), total impressions ($\mathtt{T}$), and patronage ($\mathtt{R}$) one can expect from seed sets obtained from solving the respective problem variants compared to seed sets obtained from the classical IMP variant ($\mathtt{F}$). In particular we are interested in the relative gaps between $\hat{\sigma}_{\mathtt{M}}(\hat{S}^*_{\mathtt{M}})$ and $\hat{\sigma}_{\mathtt{M}}(\hat{S}^*_{\mathtt{F}})$. Here, $\hat{S}^*_{\mathtt{M}}$ denotes the seed set obtained by solving problem variant $\mathtt{M} \in \{\mathtt{O}, \mathtt{T}, \mathtt{R}\}$, $\hat{S}^*_{\mathtt{F}}$ denotes the seed set obtained from solving variant $\mathtt{F}$, and $\hat{\sigma}_{\mathtt{M}}(\hat{S}^*_{\mathtt{F}})$ denotes the objective value obtained from evaluating $\hat{S}^*_{\mathtt{F}}$ on metric $\mathtt{M}$. Note that $\hat{\sigma}_{\mathtt{M}}(\hat{S}^*_{\mathtt{M}}) \geq \hat{\sigma}_{\mathtt{M}}(\hat{S}^*_{\mathtt{F}})$. For more fine-grained insights on variant $\mathtt{R}$, we consider three variants in which 25%, 50%, and 75% of the nodes are resistant, denoted as `R25`, `R50`, and `R75`, respectively. Resistant nodes are chosen randomly while ensuring that resistant nodes in `R25` are also resistant in `R50` whereas resistant nodes therein are also resistant in `R75`.

We further provide insights from cross-evaluating seed sets obtained from all problem variants on all other metrics. To compare these results, we compute the relative gaps $Q(\mathtt{M}, \mathtt{M}')$ between $\hat{\sigma}_{\mathtt{M}}(\hat{S}^*_{\mathtt{M}})$ and $\hat{\sigma}_{\mathtt{M}}(\hat{S}^*_{\mathtt{M}'})$ for all $\mathtt{M}, \mathtt{M}' \in \{\mathtt{F}, \mathtt{O}, \mathtt{T}, \mathtt{R25}, \mathtt{R50}, \mathtt{R75}\}$ which can be interpreted as the improvement of solving variant $\mathtt{M}$ instead of variant $\mathtt{M}'$ measured in the metric used in variant $\mathtt{M}$. For instance, to compare the improvement in the organic reach when solving variant $\mathtt{O}$ instead of solving the classical IMP (variant $\mathtt{F}$) we compute

$$Q(\mathtt{O}, \mathtt{F}) = \frac{\hat{\sigma}_{\mathtt{O}}(\hat{S}^*_{\mathtt{O}}) - \hat{\sigma}_{\mathtt{O}}(\hat{S}^*_{\mathtt{F}})}{\hat{\sigma}_{\mathtt{O}}(\hat{S}^*_{\mathtt{F}})}\,.$$

Figure 6 illustrates ratios $Q(\mathtt{M}, \mathtt{M}')$ in percent. We, however, removed five solutions in which the best seed set found was not optimal in the corresponding SAA iteration (three **`tw-naturelovers`** ($\mathtt{O}$), and two **`tw-organicfood`** ($\mathtt{R25}$)). We further remark that each column in each subfigure shows the results over all instances and $k \in \{5, 10, 15\}$ since we did not find important insights from further unraveling them. Note that in each subplot of Figure 6 there exists a column in which all values are 0%. That is, when we evaluate a seed set obtained from a certain problem variant on its own metric. Although this information is redundant, we kept such columns in the figures to ease comparison. Further note that we cut off all values above 250%, however, we report the number of cut-off outliers in the brackets over each boxplot. Finally we remark, whenever we evaluate a seed set on metric $\mathtt{F}$, we deduct the respective seed set cardinality to obtain a fair comparison.

We observe from Figure 6a that using our proposed IMP variants can lead to significant improvements in objective values compared to the classical IMP. In other words, the seed sets obtained from the classical IMP maximizing the expected number of active nodes do not perform well with respect to the considered alternative metrics accounting for passive viewing events. In instance **`tw-traveling`** extreme cases appear in which these improvements are up to 1 300%. We observe improvements of 36% on average (with a median of 19%) when excluding all results for this instance.

Figures 6b-6f show that one should use the classic IMP only when maximizing the expected number of active nodes is crucial while reaching a substantial smaller number of viewing nodes is acceptable. Indeed, these figures show that the expected numbers of active nodes obtained from problem variant $\mathtt{F}$ are much higher than those from re-evaluating seed sets obtained by other metrics. These results do, however, also reveal another advantage of considering passive viewing events. We observe that the seed sets obtained from considering one of the IMP variants different from $\mathtt{F}$ provide high-quality solutions not only on the respective metric, but also when re-evaluating them on another metric from $\{\mathtt{O}, \mathtt{T}, \mathtt{R}\}$. For example, the average improvements of using metric $\mathtt{T}$

or R instead of re-evaluating the optimal seed sets obtained for variant O are relatively small. That is, seed sets optimizing the expected organic reach also perform well w.r.t. the expected number of impressions and the expected patronage.

Figure 6: Improvements from cross-evaluating seed sets obtained from different models.

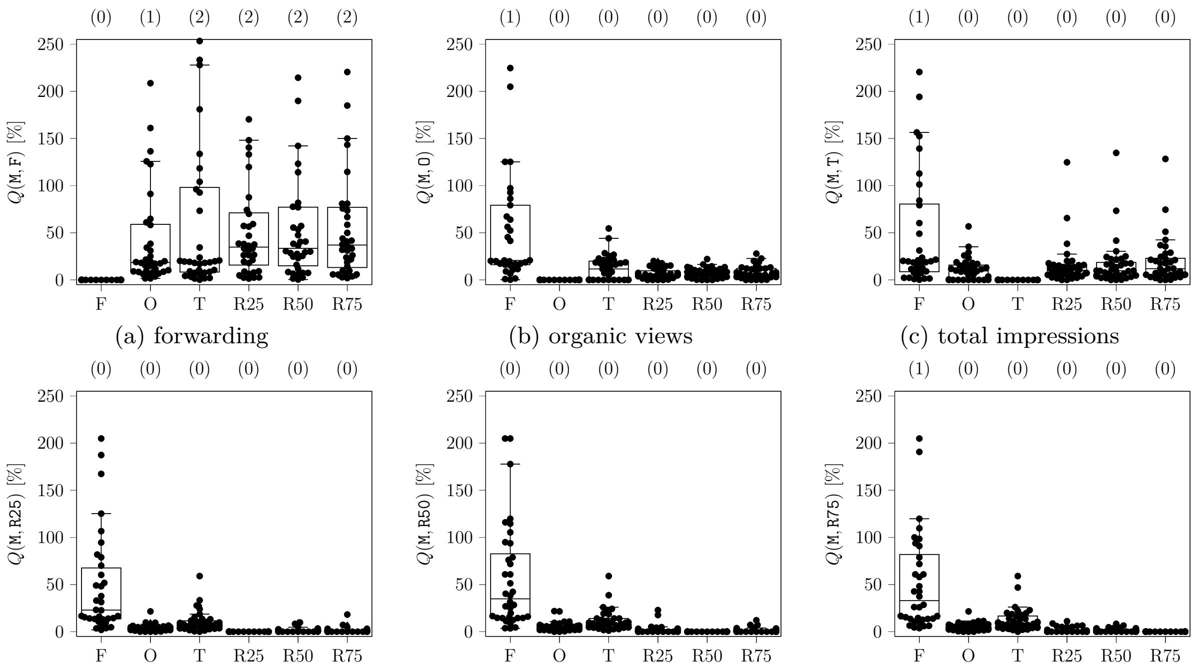

(a) forwarding (b) organic views (c) total impressions

(d) 25% resistant nodes (e) 50% resistant nodes (f) 75% resistant nodes

Note: The number of cut-off outliers is indicated in the brackets $(\cdot)$ above each boxplot.

7.6 Length of propagation cascades

Goel et al. [17] and Goel et al. [18] observe that propagation cascades are typically short which we confirm in Figure 7. The average expected depths of propagation trees $\mathbb{E}[d(T)]$ are measured in number of activation arcs $(i, j) \in \underline{A}^{\omega}$ starting from one seed node $i \in \hat{S}$ with respect to set Ω'' are depicted. Observe that the longest average propagation cascades can be expected from solving problem variant F. However, the potentially large improvements in terms of expected organic reach, expected number of total impressions, and expected patronage, (cf., Figure 6a) indicate that considering both active and passive nodes seems more important for marketing campaigns than aiming for long propagation cascades.

8 Conclusions

We have introduced and studied three new variants of the *influence maximization problem* (IMP), namely maximization of the expected organic reach (O), expected number of total impressions (T), and expected patronage (R). Main novelties include the consideration of passive viewing events, node resistance, and customer choice behavior. We showed that the considered IMP variants are NP-hard and that the precise evaluation of their (non)linear objective functions is #P-hard. We

Figure 7: Average expected propagation tree depth.

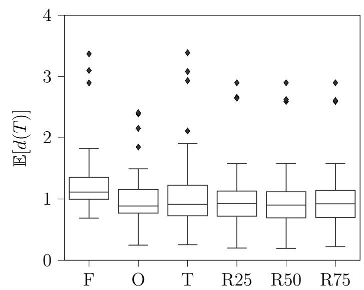

also proposed mixed-integer (non)linear programming models for the proposed IMP variants. Two linearizations of the latter models have been developed that are based on outer approximation and generalized Benders decomposition. Further theoretical results obtained show that the considered objective functions are non-monotone and submodular. Based on the latter properties we have also proven worst-case bounds for polynomial time algorithms of the proposed problem variants.

An extensive computational study has been performed on instances obtained from the social network Twitter as well as on instances from the literature. Our results show that one can obtain large improvements in terms of important marketing metrics if the problem variants proposed in this work are used instead of the classical approach. We have also shown that our approach outperforms state-of-the-art heuristics in terms of objective values but also in terms of runtimes on some instances.

Our results can serve as a base for the development of new tools for decision-making in the context of influencer marketing. The fact that influential nodes are typically interested in remuneration in practice does not restrict the application of the proposed MI(N)LP models and methods. One could, for instance, associate certain costs c_i to nodes $i \in V$ representing the incentives that influencers want to receive to act as seed nodes. In addition, the cardinality constraint (8b) can be replaced by a more general budget-constraint. Notice that this adaptation does not noteworthy influence our algorithmic developments based on MI(N)LP reformulations. In particular, the derivation of the generalized Benders cuts remain the same.

Acknowledgment

This work has been supported by the Federal Ministry of Education, Science and Research of Austria, and by the Austrian Agency for International Mobility and Cooperation in Education, Science and Research (reference number ICM-2019-13384). We further thank Ulrich Pferschy for pointing to the argument of the proof of Theorem 4 for variant `T` in personal communication.

References

[1] George Baltas and Peter Doyle. Random utility models in marketing research: a survey. *Journal of Business Research*, 51(2):115 – 125, 2001.

[2] Suman Banerjee, Mamata Jenamani, and Dilip Kumar Pratihar. A survey on influence maximization in a social network. *Knowledge and Information Systems*, pages 1–39, 2020.

[3] Gisela M. Bardossy and S. Raghavan. An inexact sample average approximation approach for the stochastic connected facility location problem. *Networks*, 70(1):19–33, 2017.

[4] Shishir Bharathi, David Kempe, and Mahyar Salek. Competitive influence maximization in social networks. In *International Workshop on Web and Internet Economics*, pages 306–311. Springer, 2007.

[5] Robert M. Bond, Christopher J. Fariss, Jason J. Jones, Adam DI Kramer, Cameron Marlow, Jaime E. Settle, and James H. Fowler. A 61-million-person experiment in social influence and political mobilization. *Nature*, 489(7415):295, 2012.

[6] Tim Carnes, Chandrashekhar Nagarajan, Stefan M. Wild, and Anke Van Zuylen. Maximizing influence in a competitive social network: a follower's perspective. In *Proceedings of the ninth international conference on Electronic commerce*, pages 351–360. ACM, 2007.

[7] Wei Chen, Chi Wang, and Yajun Wang. Scalable influence maximization for prevalent viral marketing in large-scale social networks. In *Proceedings of the 16th ACM SIGKDD International Conference on Knowledge Discovery and Data Mining*, KDD '10, pages 1029–1038, 2010.

[8] Stefano Coniglio, Fabio Furini, and Ivana Ljubić. Submodular maximization of concave utility functions composed with a set-union operator with applications to maximal covering location problems. *Mathematical Programming*, 196(1):9–56, 2022.

[9] Brian Dean. Ad blocker usage and demographic statistics in 2022, 2021. https://backlinko.com/ad-blockers-users, last accessed on 2023/01/09.

[10] Marco A Duran and Ignacio E Grossmann. An outer-approximation algorithm for a class of mixed-integer nonlinear programs. *Mathematical Programming*, 36(3):307–339, 1986.

[11] Xiao Fang, Paul Jen-Hwa Hu, Zhepeng Li, and Weiyu Tsai. Predicting adoption probabilities in social networks. *Information Systems Research*, 24(1):128–145, 2013.

[12] Golnoosh Farnad, Behrouz Babaki, and Michel Gendreau. A unifying framework for fairness-aware influence maximization. In *Companion Proceedings of the Web Conference 2020*, pages 714–722, 2020.

[13] Matteo Fischetti, Michael Kahr, Markus Leitner, Michele Monaci, and Mario Ruthmair. Least cost influence propagation in (social) networks. *Mathematical Programming*, 170(1):293–325, 2018.

[14] Roger Fletcher and Sven Leyffer. Solving mixed integer nonlinear programs by outer approximation. *Mathematical programming*, 66(1-3):327–349, 1994.

[15] Arthur M. Geoffrion. Generalized Benders decomposition. *Journal of Optimization Theory and Applications*, 10(4):237–260, 1972.

[16] Werner Geyser. The state of influencer marketing 2022: Benchmark report, 2022. https://influencermarketinghub.com/influencer-marketing-benchmark-report/, last accessed on 2022/07/20.

[17] Sharad Goel, Duncan J. Watts, and Daniel G. Goldstein. The structure of online diffusion networks. In *Proceedings of the 13th ACM Conference on Electronic Commerce*, EC '12, pages 623–638, New York, NY, USA, 2012. Association for Computing Machinery.

[18] Sharad Goel, Ashton Anderson, Jake Hofman, and Duncan J. Watts. The structural virality of online diffusion. *Management Science*, 62(1):180–196, 2016.

[19] Mark Granovetter. Threshold models of collective behavior. *The American Journal of Sociology*, 83(6):1420–1443, 1978.

[20] Evren Güney, Markus Leitner, Mario Ruthmair, and Markus Sinnl. Large-scale influence maximization via maximal covering location. *European Journal of Operational Research*, 289 (1):144–164, 2020.

[21] Dilek Günneç, Subramanian Raghavan, and Rui Zhang. Least-cost influence maximization on social networks. *INFORMS Journal on Computing*, 32(2):289–302, 2020.

[22] Dilek Günneç, Subramanian Raghavan, and Rui Zhang. A branch-and-cut approach for the least cost influence problem on social networks. *Networks*, 76(1):84–105, 2020.

[23] Dorit S. Hochbaum and Anu Pathria. Analysis of the greedy approach in problems of maximum k-coverage. *Naval Research Logistics*, 45(6):615–627, 1998.

[24] Akshay Java, Pranam Kolari, Tim Finin, Tim Oates, et al. Modeling the spread of influence on the blogosphere. *UMBC TR-CS-06-03*, 2006.

[25] Michael Kahr, Markus Leitner, Mario Ruthmair, and Markus Sinnl. Benders decomposition for competitive influence maximization in (social) networks. *Omega*, 100:102264, 2021.

[26] Michael Kahr, Markus Leitner, and Ivana Ljubić. The impact of passive social media viewers in influence maximization, 2024. Available for download at https://github.com/INFORMSJoC/2023.0047.

[27] William Karush. Minima of functions of several variables with inequalities as side conditions. Master's thesis, Department of Mathematics, University of Chicago, Chicago, IL, USA, 1939.

[28] Michal Kaut and Stein W. Wallace. Evaluation of scenario-generation methods for stochastic programming. *Pacific Journal of Optimization*, 3(2):257–271, 2007.

[29] David Kempe, Jon Kleinberg, and Éva Tardos. Maximizing the spread of influence through a social network. In *Proceedings of the 9th ACM SIGKDD International Conference on Knowledge Discovery and Data Mining*, pages 137–146. ACM, 2003.

[30] David Kempe, Jon Kleinberg, and Éva Tardos. Maximizing the spread of influence through a social network. *Theory of Computing*, 11(4):105–147, 2015.

[31] M. Emre Keskin and Mehmet Güray Güler. Influence maximization in social networks: an integer programming approach. *Turkish Journal of Electrical Engineering & Computer Sciences*, 26(6):3384–3397, 2018.

[32] Anton J. Kleywegt, Alexander Shapiro, and Tito Homem-de Mello. The sample average approximation method for stochastic discrete optimization. *SIAM Journal on Optimization*, 12 (2):479–502, 2002.

[33] Mandy Korpusik, Shigeyuki Sakaki, Francine Chen, and Yan-Ying Chen. Recurrent neural networks for customer purchase prediction on twitter. *CBRecSys@ RecSys*, 1673:47–50, 2016.

[34] Michal Kosinski, David Stillwell, and Thore Graepel. Private traits and attributes are predictable from digital records of human behavior. *Proceedings of the National Academy of Sciences*, 110(15):5802–5805, 2013.

[35] Harold W. Kuhn and Albert W. Tucker. Nonlinear programming. In *Proceedings of the Second Berkeley Symposium on Mathematical Statistics and Probability*, pages 481–492. University of California Press, 1951.

[36] Alex Leavitt, Evan Burchard, David Fisher, and Sam Gilbert. The influentials: New approaches for analyzing influence on twitter. *Web Ecology Project*, 4(2):1–18, 2009.

[37] Matthew K.O. Lee, Na Shi, Christy M.K. Cheung, Kai H. Lim, and Choon Ling Sia. Consumer's decision to shop online: The moderating role of positive informational social influence. *Information & Management*, 48(6):185–191, 2011.

[38] Jure Leskovec and Andrej Krevl. SNAP Datasets: Stanford large network dataset collection, 2014. http://snap.stanford.edu/data, last accessed on 2019/12/12.

[39] Yishi Lin and John C.S. Lui. Analyzing competitive influence maximization problems with partial information: An approximation algorithmic framework. *Performance Evaluation*, 91: 187–204, 2015.

[40] Dong Liu, Yun Jing, Jing Zhao, Wenjun Wang, and Guojie Song. A fast and efficient algorithm for mining top-k nodes in complex networks. *Scientific Reports*, 7(1), 2017.

[41] Tien Mai and Andrea Lodi. A multicut outer-approximation approach for competitive facility location under random utilities. *European Journal of Operational Research*, 284(3):874–881, 2020.

[42] Daniel McFadden. Conditional logit analysis of qualitative choice behaviour. In P. Zarembka, editor, *Frontiers in Econometrics*, pages 105–142. Academic Press New York, New York, NY, USA, 1973.

[43] Daniel McFadden. The choice theory approach to market research. *Marketing science*, 5(4): 275–297, 1986.

[44] George L. Nemhauser, Laurence A. Wolsey, and Marshall L. Fisher. An analysis of approximations for maximizing submodular set functions. *Mathematical Programming*, 14(1):265–294, 1978.

[45] Mark Newman. *Networks: An Introduction*. Oxford University Press, USA, 1 edition, 2010.

[46] Huy Nguyen and Rong Zheng. On budgeted influence maximization in social networks. *IEEE Journal on Selected Areas in Communications*, 31(6):1084–1094, 2013.

[47] Lawrence Page, Sergey Brin, Rajeev Motwani, and Terry Winograd. The pagerank citation ranking: Bringing order to the web. Technical report, Stanford InfoLab, 1999.

[48] Jürgen Pfeffer, Daniel Matter, and Anahit Sargsyan. The half-life of a tweet. *Proceedings of the International AAAI Conference on Web and Social Media*, 17(1):1163–1167, 2023.

[49] Ignacio Quesada and Ignacio E Grossmann. An lp/nlp based branch and bound algorithm for convex minlp optimization problems. *Computers & Chemical Engineering*, 16(10-11):937–947, 1992.

[50] Subramanian Raghavan and Rui Zhang. A branch-and-cut approach for the weighted target set selection problem on social networks. *INFORMS Journal on Optimization*, 1(4):304–322, 2019.

[51] Subramanian Raghavan and Rui Zhang. Weighted target set selection on trees and cycles. *Networks*, 77(4):587–609, 2021.

[52] Subramanian Raghavan and Rui Zhang. Rapid influence maximization on social networks: The positive influence dominating set problem. *INFORMS Journal on Computing*, 34(3): 1345–1365, 2022.

[53] Subramanian Raghavan and Rui Zhang. Influence maximization with latency requirements on social networks. *INFORMS Journal on Computing*, 34(2):710–728, 2022.

[54] Fabián Riquelme and Pablo González-Cantergiani. Measuring user influence on twitter: A survey. *Information processing & management*, 52(5):949–975, 2016.

[55] Ryan A. Rossi and Nesreen K. Ahmed. The network data repository with interactive graph analytics and visualization. In *Proceedings of the 29th AAAI Conference on Artificial Intelligence*, 2015. http://networkrepository.com, last accessed on 2019/12/12.

[56] Alexander Schrijver. *Combinatorial optimization: polyhedra and efficiency*, volume 24. Springer Science & Business Media, 2003.

[57] Shashank Sheshar Singh, Kuldeep Singh, Ajay Kumar, Harish Kumar Shakya, and Bhaskar Biswas. A survey on information diffusion models in social networks. In Ashish Kumar Luhach, Dharm Singh, Pao-Ann Hsiung, Kamarul Bin Ghazali Hawari, Pawan Lingras, and Pradeep Kumar Singh, editors, *Advanced Informatics for Computing Research*, pages 426–439, 2019.

[58] Xinfang Song, Wei Jiang, Xiaohui Liu, Hui Lu, Zhihong Tian, and Xiaojiang Du. A survey of game theory as applied to social networks. *Tsinghua Science and Technology*, 25(6):734–742, 2020.

[59] Tricia Stone. The truth about using facebook to market your business. *Journal of Financial Planning*, 32(9):42–43, 09 2019.

[60] Joffre Swait and Jordan Louviere. The role of the scale parameter in the estimation and comparison of multinomial logit models. *Journal of Marketing Research*, 30(3):305–314, 1993.

[61] Kübra Tanınmış, Necati Aras, and IK Altınel. Influence maximization with deactivation in social networks. *European Journal of Operational Research*, 278(1):105 – 119, 2019.

[62] Michael Trusov, Randolph E. Bucklin, and Koen Pauwels. Effects of word-of-mouth versus traditional marketing: Findings from an internet social networking site. *Journal of Marketing*, 73(5):90–102, 2009.

[63] Daniel Tunkelang. A twitter analog to pagerank, 2009. https://thenoisychannel.com/2009/01/13/a-twitter-analog-to-pagerank, last accessed on 2020/08/24.

[64] Dan Virgillito. Which social media platforms offer the greatest organic reach?, 2016. https://www.elegantthemes.com/blog/resources/which-social-media-platforms-offer-the-greatest-organic-reach, last accessed on 2020/09/28.

[65] Stanley Wasserman, Katherine Faust, et al. *Social network analysis: Methods and applications*, volume 8. Cambridge University Press, 1994.

[66] Hao-Hsiang Wu and Simge Küçükyavuz. A two-stage stochastic programming approach for influence maximization in social networks. *Computational Optimization and Applications*, 69 (3):563–595, 2018.

This appendix is structured as follows: A contains the proofs of all statements of the main article. B details the separation of Benders cuts for integer candidate solutions. C provides additional and detailed computational results. D discusses results obtained from solving our proposed CIMP variant. Finally, E includes further information about the instances used.

A Proofs

The following results discuss submodularity properties of different problem variants. To this end, recall that a real-valued function $f(\cdot)$ defined on a finite ground-set D is submodular if $f(\emptyset) = 0$ and if $f(A) + f(B) \geq f(A \cup B) + f(A \cap B)$ holds for any $A \subseteq D$ and $B \subseteq D$. The marginal gain of adding an element i to set A is denoted by $\varrho_i^f(A)$ and is defined as $f(A \cup \{i\}) - f(A)$. Function f is said to be monotone if $f(A') \leq f(A)$, for any $A' \subset A$.

Proof. Function $\mathcal{R}_\omega(S)$ is the set-union operator, and hence its cardinality is a submodular function [56, Section 44]. The marginal gain of adding an extra node i into S can be negative if $i \in \mathcal{R}_\omega(S)$, because then $|\mathcal{R}_\omega(S) \setminus S| > |\mathcal{R}_\omega(S) \setminus \{S \cup \{i\}\}|$. Hence, the latter function is non-monotone. $\square$

Proof. We first observe that the function $\sigma_{\mathrm{T}}^\omega(S)$ can be restated as

$$\sigma_{\mathrm{T}}^\omega(S) = \sum_{j \in V \setminus S} \nu_j^\omega(S)$$

where function $\nu_j^\omega(S)$ counts the number of views of node j induced by the set $S \subseteq V$. It is sufficient to show that function $\nu_j^\omega(S)$ is submodular with respect to S for an arbitrary node $j \in V \setminus S$, for a given scenario $\omega \in \Omega$. This follows from the fact that $\mathcal{A}_\omega(S)$ is a set-union operator applied to nodes $\mathcal{N}_\omega^-(j)$ because $\nu_j^\omega(S) = |\mathcal{A}_\omega(S) \cap \mathcal{N}_\omega^-(j)|$. To show non-monotonicity consider an arbitrary node

$j \notin S$ that has only one incident viewing arc $(i,j) \in A^\omega \setminus \underline{A}^\omega$ and $i \in \mathcal{A}_\omega(S)$. Then, adding node j to S reduces the objective function value w.r.t. set S by one, i.e., $\sigma^\omega_{\mathtt{T}}(S \cup \{j\}) = \sigma^\omega_{\mathtt{T}}(S) - 1$. $\square$

Proof. We exploit the fact that the function $\nu^\omega_j(S)$, counting the number of views for a node j is submodular (see the proof of Theorem 2), together with the fact that the function $g(x) = \frac{x}{x+r}$, is strictly increasing and concave for $r > 0$ and $x \geq 0$. A composition of an increasing concave function and a submodular function preserves submodularity, and so is the resulting function, denoted by $h^\omega_j(S) = g(\nu^\omega_j(S))$ submodular. Moreover, any non-negative linear combination of submodular functions preserves submodularity. Thus, $\sigma^\omega_{\mathtt{R}}(S) = \sum_{j \in V \setminus S} h^\omega_j(S)$ is submodular. Non-monotonicity is implied by repeating the argument given in the proof of Theorem 2. $\square$

Proof. We show the statements for variants R and O by observing that problem variant R contains the IMP as a special case. Consider an arbitrary instance of the IMP defined on graph $G = (V, A)$ with (forwarding) activation probabilities $p_{ij} \in [0, 1]$, for all $(i, j) \in A$, in which the seed set can contain at most $k \in \mathbb{N}$ nodes. Next, create an instance of the variant R defined on the same graph $G = (V, A)$ such that forwarding and viewing probabilities correspond to activation probabilities of the IMP (i.e., $p^{\mathrm{f}}_{ij} = p^{\mathrm{v}}_{ij} = p_{ij}$, for all $(i, j) \in A$), no node is resistant (i.e., $r_i = \varepsilon$, for all $i \in V$, for an arbitrary small $\varepsilon > 0$), and the budget is equal to k (i.e., $|S| \leq k$). It is easy to see that for arbitrary small resistance values, the fraction in the objective function (8a) corresponding to a particular node $i \in V$ and scenario $\omega \in \Omega$ is either approximately one or equal to zero depending whether or not node i is views content at least once in scenario ω. Thus, the objective function maximizes the expected organic reach O. The chosen forwarding and viewing probabilities induce that the latter number is identical to the expected number of activated nodes and thus, the optimal solution to the instance for variants R, O, defined above solve the original IMP instance, i.e., variant F. For variant T, we adapt the instance of the of variant R defined above as follows. Each node $i \in V$ gets attached dummy outneighbors $j \in \mathcal{D}(i)$ such that $|\mathcal{D}(i)| = M \in \mathbb{N}$, and $p^{\mathrm{f}}_{ij} = p^{\mathrm{v}}_{ij} = 1$ for all $i \in V$ and $j \in \mathcal{D}(i)$. Let $V' = \cup_{i \in V} \mathcal{D}(i)$, $A' = \{(i, j) : i \in V, j \in \mathcal{D}(i)\}$, and $G' = (V \cup V', A \cup A')$. For sufficiently large values of M, e.g., $|V|^2$, counting views along arcs from set A is negligible compared to those along arcs from set A'. Thus, solving variant T on G' solves the original IMP on G. The result follows since the IMP is known to be NP-hard [29]. Chen et al. 7 showed that the evaluation of the objective function of an IMP is #P-hard under the independent cascade model (cf., Kempe et al. 29). Thus, it suffices to observe that the latter model is a special case of the CIC model by the previous manipulations. To show that the evaluation of the functions $\sigma^\omega_X(S)$ can be done in $\mathcal{O}(|A|)$ time, observe that for each variant the following node sets need to be inspected: (i) activation set $\mathcal{A}_\omega(S)$ which runs in $\mathcal{O}(|A|)$, and (ii) either the set of in-neighbors $\mathcal{N}^-_\omega(i)$ or the set of out-neighbors $\mathcal{N}_\omega(i)$ (because $\mathcal{R}_\omega(S) = \mathcal{N}_\omega(\mathcal{A}_\omega(S))$) for all $i \in V$, respectively, which runs in $\mathcal{O}(|A|)$. $\square$

Proof. First note that the objective function (8a) is monotone increasing in variables $\mathbf{v}$. Thus, constraints (8c) and (8d) are tight which is ensured by the latter monotonicity. The coordinates of $\mathbf{y}^* \in P_{\mathbf{y}}$ are integral by definition, thus, this also holds for $\mathbf{f}^*$ and $\mathbf{v}^*$. $\square$

Proof. We first rewrite formulation (13) explicitly into one master problem (15) and $|\Omega|$ subproblems (16):

$$
\begin{aligned}
\text{(GB)} \quad \max \quad & \sum_{\omega \in \Omega} p^{\omega} u^{\omega} && && \text{(15a)}\\
\text{s.t.} \quad & u^{\omega} \leq \Phi^{\omega}(\mathbf{y}) && \forall \omega \in \Omega && \text{(15b)}\\
& \mathbf{y} \in P_{\mathbf{y}}
\end{aligned}
$$

where

$$
\begin{aligned}
\Phi^{\omega}(\mathbf{y}) \quad = \quad \max_{\mathbf{v},\mathbf{f}} \quad & \sum_{i \in V} \frac{b_i v_i^{\omega}}{b_i v_i^{\omega} + r_i} && && && \text{(16a)}\\
\text{s.t.} \quad & \sum_{j \in \mathcal{N}_{\omega}^{-}(i)} f_j^{\omega} \geq v_i^{\omega} && (\alpha_i^{\omega}) && \forall i \in V && \text{(16b)}\\
& \sum_{j \in \mathcal{A}_{\omega}^{-}(i)} y_j \geq f_i^{\omega} && (\beta_i^{\omega}) && \forall i \in V && \text{(16c)}\\
& v_i^{\omega} \leq |\mathcal{N}_{\omega}^{-}(i)|(1 - y_i) && (\varphi_i^{\omega}) && \forall i \in V && \text{(16d)}\\
& f_i^{\omega} \leq 1 && (\gamma_i^{\omega}) && \forall i \in V && \text{(16e)}
\end{aligned}
$$

The function $\Phi^{\omega}(\mathbf{y})$ is concave for each scenario $\omega \in \Omega$. Therefore, it can be overestimated by first-order approximations based on tangential hyperplanes derived from its supergradients. Hence, the following sequence of inequalities holds

$$
u^{\omega} \leq \Phi^{\omega}(\mathbf{y}) \leq \Phi^{\omega}(\bar{\mathbf{y}}) + \bar{\boldsymbol{\rho}}^{\omega\intercal}(\mathbf{y} - \bar{\mathbf{y}}) \qquad \forall \bar{\mathbf{y}} \in P_{\mathbf{y}}, \forall \omega \in \Omega\,.
$$

whereby the right-most term corresponds to a supporting hyperplane at $\bar{\mathbf{y}} \in P_{\mathbf{y}}$ in each scenario $\omega \in \Omega$. We now derive the coordinates of supergradients $\bar{\boldsymbol{\rho}}^{\omega}$ via the partial derivatives of the Lagrangian relaxation of (16) with respect to $\mathbf{y}$ which we detail now for a specific scenario $\omega \in \Omega$. Let $\mathcal{L}^{\omega}(\bar{\mathbf{y}}, \mathbf{f}^{\omega}, \mathbf{v}^{\omega}, \boldsymbol{\alpha}^{\omega}, \boldsymbol{\beta}^{\omega}, \boldsymbol{\varphi}^{\omega}, \boldsymbol{\gamma}^{\omega})$ denote the aforementioned Lagrangian abbreviated by $\mathcal{L}^{\omega}(\cdot)$ so that

$$
\begin{aligned}
\mathcal{L}^{\omega}(\cdot) = \quad & \sum_{i \in V} \frac{b_i v_i^{\omega}}{b_i v_i^{\omega} + r_i} + \alpha_i^{\omega}\Big(\sum_{j \in \mathcal{N}_{\omega}^{-}(i)} f_j^{\omega} - v_i^{\omega}\Big) + \beta_i^{\omega}\Big(\sum_{j \in \mathcal{A}_{\omega}^{-}(i)} \bar{y}_j - f_i^{\omega}\Big)\\
& + \varphi_i^{\omega}\big(|\mathcal{N}_{\omega}^{-}(i)|(1 - \bar{y}_i) - v_i^{\omega}\big) + \gamma_i^{\omega}(1 - f_i^{\omega}), \qquad \text{(17)}
\end{aligned}
$$

where $[\boldsymbol{\alpha}^{\omega\intercal}\, \boldsymbol{\beta}^{\omega\intercal}\, \boldsymbol{\varphi}^{\omega\intercal}\, \boldsymbol{\gamma}^{\omega\intercal}]^{\intercal} \geq \mathbf{0}$, are the dual variables associated to constraints (16b), (16c), (16d), and (16e), respectively. We can use the Karush-Kuhn-Tucker (KKT) conditions [27, 35] because the objective function in (16) is concave and all constraints are linear therein, thus, strong duality holds which is the key argument in this proof. Then, the coordinates of the corresponding supergradient are derived by

$$
\frac{\partial \mathcal{L}^{\omega}(\cdot)}{\partial y_i} = \bar{\rho}_i^{\omega} = \sum_{j \in \mathcal{A}_{\omega}(i)} \bar{\beta}_j^{\omega} - |\mathcal{N}_{\omega}^{-}(i)| \bar{\varphi}_i^{\omega} \qquad \forall i \in V, \qquad \text{(18)}
$$

where $\bar{\boldsymbol{\beta}}^{\omega}$ and $\bar{\boldsymbol{\varphi}}^{\omega}$ represent the optimal dual multipliers in (17). Thus, to identify these optimal values we impose the corresponding KKT conditions:

$$
\frac{\partial \mathcal{L}^{\omega}(\cdot)}{\partial f_i^{\omega}} = 0 \implies \sum_{j \in \mathcal{N}_{\omega}(i)} \alpha_j^{\omega} = \beta_i^{\omega} + \gamma_i^{\omega} \qquad \forall i \in V \qquad \text{(19a)}
$$

$$\frac{\partial \mathcal{L}^\omega(\cdot)}{\partial v_i^\omega} = 0 \implies \frac{b_i r_i}{(b_i v_i^\omega + r_i)^2} = \alpha_i^\omega + \varphi_i^\omega \qquad \forall i \in V \tag{19b}$$

$$\alpha_i^\omega \Big(\sum_{j \in \mathcal{N}_\omega^-(i)} f_j^\omega - v_i^\omega \Big) = 0 \qquad \forall i \in V \tag{19c}$$

$$\beta_i^\omega \Big(\sum_{j \in \mathcal{A}_\omega^-(i)} \bar{y}_j - f_i^\omega \Big) = 0 \qquad \forall i \in V \tag{19d}$$

$$\varphi_i^\omega (|\mathcal{N}_\omega^-(i)|(1-\bar{y}_i) - v_i^\omega) = 0 \qquad \forall i \in V \tag{19e}$$

$$\gamma_i^\omega (1 - f_i^\omega) = 0 \qquad \forall i \in V \tag{19f}$$

We again exploit the monotonicity of objective function (16a) and the structure of constraints (16b), (16c) and (16d) for the computation of all variable values at any point $\bar{\mathbf{y}} \in P_{\mathbf{y}}$. That is, $\bar{f}_i^\omega = \min\{1, \sum_{j \in \mathcal{A}_\omega^-(i)} \bar{y}_j\}$ and $\bar{v}_i^\omega = \min\{|\mathcal{N}_\omega^-(i)|(1-\bar{y}_i), \sum_{j \in \mathcal{N}_\omega^-(i)} \bar{f}_j^\omega\}$, for all $i \in V$, thus, we can compute $\Phi^\omega(\bar{\mathbf{y}})$ by inspection given any point $\bar{\mathbf{y}} \in P_{\mathbf{y}}$. We proceed with the determination of dual variables $\boldsymbol{\beta}^\omega$ and $\boldsymbol{\varphi}^\omega$. It is convenient to define first order partial derivative of function $\Phi^\omega(\bar{\mathbf{y}})$ (cf., 19b) as

$$\bar{m}_i^\omega := \frac{b_i r_i}{(b_i \bar{v}_i^\omega + r_i)^2} \qquad \forall i \in V\,,$$

i.e., the marginal gain with respect to viewing variables $\bar{\mathbf{v}}^\omega$. Let $\bar{S} = \{i \in V : \bar{y}_i = 1\}$ denote the current seed set and $\bar{V}^\omega := \{i \in V : \bar{v}_i^\omega = |\mathcal{N}_\omega^-(i)|\} \cup \{\bar{S}\}$ be the set of saturated nodes. Then, we gather that

$$\bar{\alpha}_i^\omega = \begin{cases} 0 & \text{if } i \in \bar{V}^\omega, \\ \bar{m}_i^\omega & \text{otherwise,} \end{cases} \quad \forall i \in V\,, \qquad \bar{\varphi}_i^\omega = \begin{cases} \bar{m}_i^\omega & \text{if } i \in \bar{V}^\omega, \\ 0 & \text{otherwise,} \end{cases} \quad \forall i \in V\,,$$

holds due to (19b), (19c) and (19e). Notice that for seed nodes $\bar{S}$ we can always set $\bar{\alpha}_i^\omega = 0$ by (19c) because we excluded seed set variables from contributing to the objective function, i.e., $\bar{v}_i^\omega = 0$, for all $i \in \bar{S}$ and $\omega \in \Omega$. Let $\bar{I}_i = \sum_{j \in \mathcal{A}_\omega^-(i)} \bar{y}_j$ and observe that $\bar{I}_i < 1$ implies $\bar{f}_i^\omega < 1$. Then,

$$\bar{\beta}_i^\omega = \begin{cases} \sum_{j \in \mathcal{N}_\omega(i)} \bar{\alpha}_j^\omega & \text{if } \bar{I}_i < 1, \\ 0 & \text{otherwise,} \end{cases} \quad \forall i \in V\,, \qquad \bar{\gamma}_i^\omega = \begin{cases} 0 & \text{if } \bar{I}_i < 1, \\ \sum_{j \in \mathcal{N}_\omega(i)} \bar{\alpha}_j^\omega & \text{otherwise,} \end{cases} \quad \forall i \in V\,,$$

holds due to (19a) and the complimentary slackness conditions (19d) and (19f). Notice that the latter statement also implies that $\bar{\beta}_j^\omega = 0$ for all forwarding nodes because $\bar{I}_j \geq 1$, for all $j \in \mathcal{A}_\omega(\bar{S})$. Since seed nodes forward content it holds that

$$\bar{\rho}_i^\omega = -|\mathcal{N}_\omega^-(i)|\bar{m}_i^\omega \qquad \forall i \in \bar{S}\,,$$

by (18). For nodes $i \notin \bar{S}$ we have to distinguish whether or not they are saturated, i.e., if $i \in \bar{V}^\omega$ or $i \in V \setminus \bar{V}^\omega$. Notice that the former case implies that $\mathcal{N}_\omega^-(i) \subseteq \mathcal{A}_\omega(\bar{S})$ whereas the latter case implies the existence of a node $j \in \mathcal{N}_\omega^-(i) \cap \{\mathcal{A}_\omega(i) \setminus \mathcal{A}_\omega(\bar{S})\}$. Thus, we have

$$\begin{aligned} \bar{\rho}_i^\omega = \sum_{j \in \mathcal{A}_\omega(i)} \bar{\beta}_j^\omega - |\mathcal{N}_\omega^-(i)|\bar{\varphi}_i^\omega &= \sum_{j \in \mathcal{A}_\omega(i) \setminus \mathcal{A}_\omega(\bar{S})} \sum_{k \in \mathcal{N}_\omega(j)} \bar{\alpha}_k^\omega - |\mathcal{N}_\omega^-(i)|\bar{\varphi}_i^\omega \\ &= \sum_{j \in \mathcal{A}_\omega(i) \setminus \mathcal{A}_\omega(\bar{S})} \sum_{k \in \mathcal{N}_\omega(j)} \bar{m}_k^\omega - |\mathcal{N}_\omega^-(i)|\bar{m}_i^\omega \qquad \forall i \in \bar{V}^\omega \setminus \bar{S}\,, \end{aligned}$$

and

$$\bar{\rho}_i^\omega = \sum_{j\in\mathcal{A}_\omega(i)} \bar{\beta}_j^\omega = \sum_{j\in\mathcal{A}_\omega(i)\setminus\mathcal{A}_\omega(\bar{S})} \sum_{k\in\mathcal{N}_\omega(j)} \bar{\alpha}_k^\omega = \sum_{j\in\mathcal{A}_\omega(i)\setminus\mathcal{A}_\omega(\bar{S})} \sum_{k\in\mathcal{N}_\omega(j)} \bar{m}_k^\omega \qquad \forall i \in V \setminus \bar{V}^\omega .$$

The coordinates of the supergradients are then derived by

$$\bar{\rho}_i^\omega = \begin{cases} -|\mathcal{N}_\omega^-(i)|\bar{m}_i^\omega & \text{if } i \in \bar{S} \\ \sum_{j\in\mathcal{A}_\omega(i)\setminus\mathcal{A}_\omega(\bar{S})} \sum_{k\in\mathcal{N}_\omega(j)} \bar{m}_k^\omega & \text{if } i \in V \setminus \bar{V}^\omega \\ \sum_{j\in\mathcal{A}_\omega(i)\setminus\mathcal{A}_\omega(\bar{S})} \sum_{k\in\mathcal{N}_\omega(j)} \bar{m}_k^\omega - |\mathcal{N}_\omega^-(i)|\bar{m}_i^\omega & \text{if } i \in \bar{V}^\omega \setminus \bar{S} \end{cases} \tag{20}$$

which is exactly the same as (14) which completes the proof for problem variant `R`. □

Proof. For problem variant `T`, we change the terms of the sum in (16a) and the corresponding terms in the Lagrangian (17) to v_i^ω. Consequently, the KKT conditions (19b) simplify to $\alpha_i^\omega + \varphi_i^\omega = 1$, i.e, the marginal gains $\bar{m}_i^\omega = 1$, for all $i \in V$ and $\omega \in \Omega$. □

Proof. For problem variant `O`, we augment the proof of Corollary 1 by substituting each term $|\mathcal{N}_\omega^-(i)|$ the proof of Theorem 6 with one (cf., Section 3.2). □

Proof. For problem variant `F`, we change objective function (16a) to (10) and remove viewing variables $\mathbf{v}$ and constraints (16b) and (16d) in the proof of Theorem 6. Thus, dual variables $\boldsymbol{\alpha}^\omega$ and $\boldsymbol{\varphi}^\omega$ do not exist so that we can further remove the KKT conditions (19b), (19c) and (19e) and the corresponding terms in the Lagrangian (17). Another consequence is that the first term in Lagrangian (17) changes to f_i^ω and therefore (19a) changes to $\beta_i^\omega + \gamma_i^\omega = 1$. Notice that the right-hand side of the latter expression corresponds now to the marginal gains, i.e., the first order partial derivative of the new objective function with respect to $\mathbf{f}^\omega$ so that $\bar{m}_i^\omega = 1$, for all $i \in V$ and $\omega \in \Omega$. Further notice that the set of saturated nodes $\bar{V}^\omega$ reduces to set $\bar{S}$.

Again we observe that setting $\bar{\beta}_i^\omega = 0$ and $\bar{\gamma}_i^\omega = \bar{m}_i^\omega$ for all forwarding nodes $i \in \mathcal{A}_\omega(\bar{S})$ is valid by conditions (19d) and (19f). Conversely, $\bar{\beta}_i^\omega = \bar{m}_i^\omega$ and $\bar{\gamma}_i^\omega = 0$ is valid for all non-forwarding nodes $i \in \mathcal{A}_\omega(V \setminus \bar{S}) \setminus \mathcal{A}_\omega(\bar{S})$ by the same set of KKT conditions. Thus, the supergradient coordinates can be derived by

$$\bar{\rho}_i^\omega = \begin{cases} 0 & \text{if } i \in \bar{S} \\ |\mathcal{A}_\omega(i) \setminus \mathcal{A}_\omega(\bar{S})| & \text{otherwise,} \end{cases} \qquad \forall i \in V .$$

□

Proof. This proof is based on the proof of Theorem 6 and first considers problem variant `R`. To obtain the current objective value of a specific scenario $\Phi^\omega(\bar{\mathbf{y}})$ for (possibly fractional) $\bar{\mathbf{y}} \in P'_{\mathbf{y}} := \{\mathbf{y} \in [0,1]^{|V|} : \sum_{i\in V} y_i \le k\}$ we first compute the forwarding and viewing variables by $\bar{f}_i^\omega = \min\{1, \sum_{j\in\mathcal{A}_\omega^-(i)} \bar{y}_j\}$ and $\bar{v}_i^\omega = \min\{|\mathcal{N}_\omega^-(i)|(1-\bar{y}_i), \sum_{j\in\mathcal{N}_\omega^-(i)} \bar{f}_j^\omega\}$ for all $i \in V$, respectively, and the $\Phi^\omega(\bar{\mathbf{y}})$, which runs in $\mathcal{O}(|V|^2)$. Obtaining the dual variables $\bar{\boldsymbol{\alpha}}^\omega$ and $\bar{\boldsymbol{\varphi}}^\omega$, i.e., the marginal gains

$\bar{\mathbf{m}}^\omega$, runs in $\mathcal{O}(|V|)$ whereas the computation of the dual variables $\bar{\boldsymbol{\beta}}^\omega$ and $\bar{\boldsymbol{\gamma}}^\omega$ needs $\mathcal{O}(|V|^2)$. Thus, the separation routine for one specific scenario runs in $\mathcal{O}(|V|^2)$. To see that the latter runtime also holds for problem variants F, O, and T, it suffices to observe that computing the supergradients $\bar{\boldsymbol{\beta}}^\omega$, $\omega \in \Omega$, does not increase complexity compared to variant R (cf., **??** 1–3). $\square$

Proof. Let us consider a submodular maximization problem over a ground set D, $\max_{S \subseteq D}\{f(S) : |S| \leq k\}$, such that the marginal gains for the function f are bounded from below by $-\theta$ (i.e., $\varrho_j^f(S) \geq -\theta$, for all $S \subseteq D$, $j \in D \setminus S$). Then, Theorem 4.2 of Nemhauser et al. [44] states that the MG heuristic provides a solution $\tilde{S}$ to this problem such that

$$\frac{f(S^*) - f(\tilde{S})}{f(S^*) - f(\emptyset) + k\theta} \leq \alpha^k,$$

where S^* is an optimal solution. Given that $\sigma_{\mathtt{M}}(\emptyset) = 0$ and that the bounds for marginal gains are defined as $\theta = 1$ for the variants O,R and $\theta = \max_{i \in V} |\mathcal{N}^-(i)|$ for the variant T, the result follows directly after rearranging the terms from the inequality above. $\square$

Proof. Given that $0 \leq \alpha^k < e^{-1}$ and $\theta = 1$, we can underestimate the second term of the right-hand-side of the result in Theorem 8 by $-k/e$. $\square$

Proof. Given that $0 \leq \alpha^k < e^{-1}$ and $\theta = \max_{i \in V} |\mathcal{N}^-(i)|$, we can underestimate the second term of the right-hand-side of the result in Theorem 8 by $-k/e \cdot \max_{i \in V} |\mathcal{N}^-(i)| = -M \cdot k$. $\square$

B Separation of integral Benders cuts

Algorithm 1 details the method used to separate generalized Benders cuts for integral candidate solutions.

C Detailed results

This section contains additional and more detailed results of our computational study. Figure 8 shows (relative) cumulative numbers of SAA iterations solved within a given time and corresponding optimality gaps after two hours for different numbers of considered scenarios Ω'. Here, optimality gaps are computed by (UB − OV)/UB where UB denotes the best known upper bound and OV denotes the objective value of the corresponding SAA iteration.

Tables 3 to 7 detail runtimes (in seconds) and objective function values for different models and methods discussed in this article. This data is reported for each considered instance, cardinality of the seed set ($|S| \in \{5, 10, 15\}$), and the following evaluation metrics: forwarding maximization (F), organic reach maximization (O), total impression maximization (T), and expected patronage maximization (R25, R50, R75, RX). Notice that RX corresponds to the case in which we choose the resistance values of each node completely at random; cf., Section 7.1. Further note that all reported objective values do not consider the respective contribution of the seed nodes. For each considered combination we report the results obtained from different solution methods: generalized

// Input: scenario graphs $G^\omega = (V, A^\omega)$ for all $\omega \in \Omega$, solution $(\bar{\mathbf{y}}, \bar{\boldsymbol{u}})$
// Output: set $\mathcal{C}$ containing a violated generalized Benders cut (13b) for each scenario $\omega \in \Omega$ (if exists)

$\bar{S} \leftarrow \{i \in V : \bar{y}_i = 1\}$ // current seed set
$\mathcal{C} \leftarrow \emptyset$ // set of violated Benders cuts
for $\omega \in \Omega$ **do**
    $\mathbf{v}^\omega \leftarrow \mathbf{0}$
    for $i \in \mathcal{A}_\omega(\bar{S})$ **do**
        for $j \in \mathcal{N}_\omega(i)$ **do**
            $\bar{v}_j^\omega \leftarrow \bar{v}_j^\omega + 1$
    $\bar{v}_i^\omega \leftarrow 0, \forall i \in \bar{S}$
    $\sigma_{\mathtt{R}}^\omega(\bar{S}) \leftarrow \sum_{i \in V} \frac{b_i \bar{v}_i^\omega}{b_i \bar{v}_i^\omega + r_i}$
    if $\bar{u}^\omega > \sigma_{\mathtt{R}}^\omega(\bar{S})$ // violated Benders cut
    then
        compute $\bar{\boldsymbol{\rho}}^\omega$ according to (14) // supergradient
        $\mathcal{C} \leftarrow \mathcal{C} \cup \{u^\omega \leq \sigma_{\mathtt{R}}^\omega(\bar{S}) + \sum_{i \in \bar{S}} \bar{\rho}_i^\omega (y_i - 1) + \sum_{i \notin \bar{S}} \bar{\rho}_i^\omega y_i\}$ // add cut

Algorithm 1: Separation of generalized Benders cuts for integral candidate solutions $\bar{\mathbf{y}} \in P(\mathbf{y})$.

Benders decomposition (GB), and the heuristics betweenness centrality (BC), distance centrality (DC), expected outdegree (EG), marginal gain (MG), reverse PageRank (PR), replies and mentions (RM), and TunkRank (TR). As RM and TR are geared to Twitter instances, we do not report such results for the instances from the literature, i.e., in Tables 6 and 7. All results are based on the settings $|\Omega'| = 100$.

Figure 8: Performance profiles and optimality gaps of each SAA iteration (cf., Section 7.2).

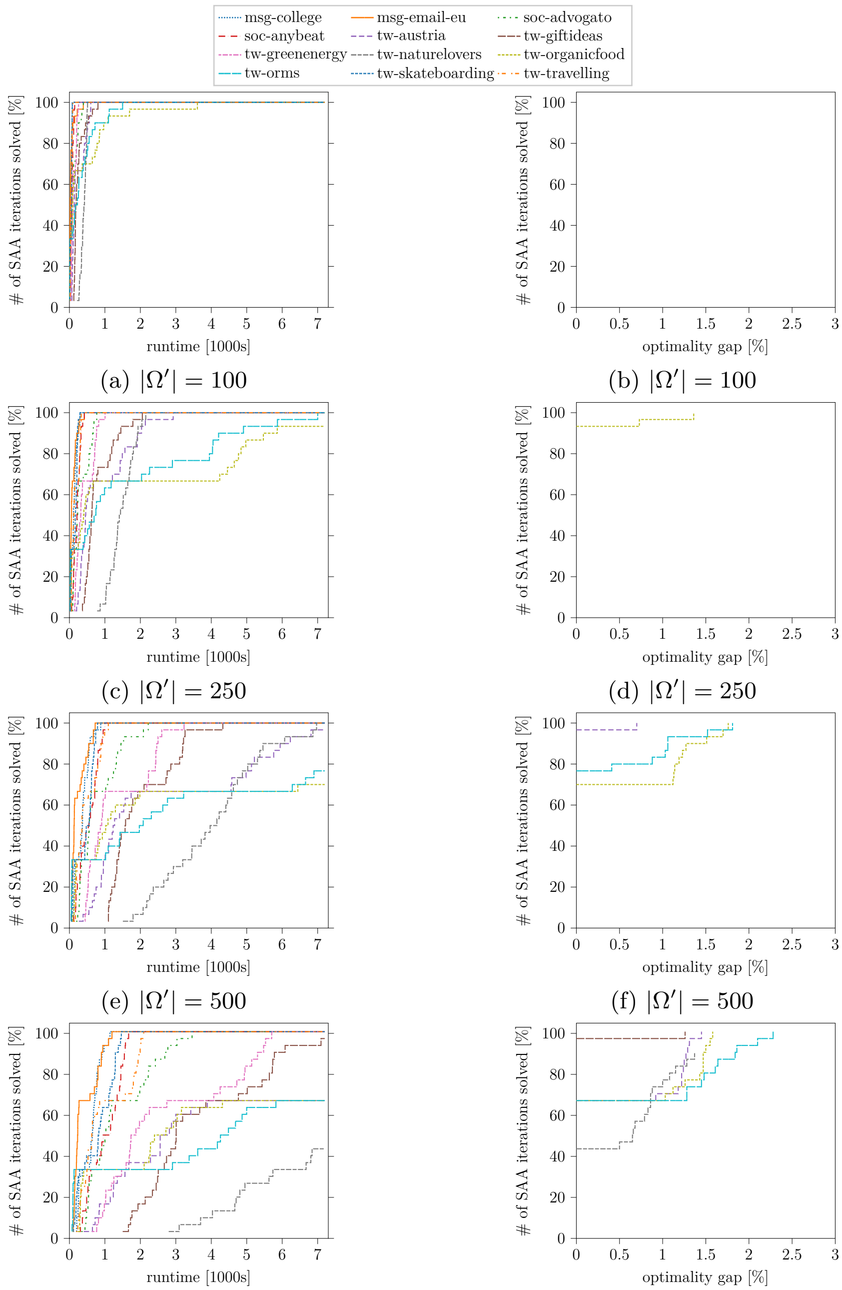

(a) $|\Omega'| = 100$ (b) $|\Omega'| = 100$

(c) $|\Omega'| = 250$ (d) $|\Omega'| = 250$

(e) $|\Omega'| = 500$ (f) $|\Omega'| = 500$

(g) $|\Omega'| = 750$ (h) $|\Omega'| = 750$

Table 3: Runtimes and objective values for instances tw-austria and tw-giftideas.

Instance	$\|S\|$	Metric	runtimes								objective values							
			GB	BC	DC	ED	MG	PR	RM	TR	GB	BC	DC	ED	MG	PR	RM	TR
tw-austria	5	F	**2**	14	0	0	60	0	0	0	**53**	4	10	10	**53**	10	30	0
		O	176	14	0	0	80	0	0	0	**1 765**	654	1 489	1 489	1 489	1 489	1 524	46
		T	1	14	**0**	**0**	62	**0**	0	0	**2 777**	728	**2 777**	**2 777**	**2 777**	**2 777**	1 918	106
		R25	103	14	0	0	**90**	0	0	0	**164**	44	129	129	**164**	129	145	5
		R50	**66**	14	0	0	90	0	0	0	**120**	31	92	92	**120**	92	106	4
		R75	**36**	14	0	0	91	0	0	0	**80**	20	62	62	**80**	62	69	3
		RX	**84**	13	0	0	89	0	0	0	**131**	36	104	104	**131**	104	115	4
	10	F	**5**	15	0	0	124	0	0	0	**70**	7	27	27	**70**	27	42	27
		O	2 228	14	0	0	152	0	0	0	**2 386**	1 175	1 965	1 965	2 069	1 965	2 124	1 052
		T	**1**	15	0	0	124	0	0	0	**4 653**	1 511	4 574	4 574	**4 653**	4 574	2 950	1 321
		R25	250	13	0	0	**187**	0	0	0	**245**	87	223	223	**245**	223	194	109
		R50	208	14	0	0	190	0	0	0	**178**	60	165	165	176	165	139	81
		R75	**125**	14	0	0	192	0	0	0	**119**	37	111	111	**119**	111	92	53
		RX	**138**	13	0	0	189	0	0	0	**196**	67	180	180	**196**	180	153	87
	15	F	**12**	15	0	0	186	0	0	0	**82**	9	32	32	**82**	33	49	47
		O	5 133	15	0	0	238	0	0	0	**2 694**	1 544	2 208	2 208	2 275	2 275	2 190	1 095
		T	**12**	15	0	0	198	0	0	0	**6 082**	2 231	6 061	6 061	**6 082**	6 080	3 271	1 377
		R25	1 530	14	0	0	284	0	0	0	**299**	110	272	272	292	276	207	117
		R50	412	13	0	0	286	0	0	0	**219**	77	200	200	215	203	148	87
		R75	304	13	0	0	294	0	0	0	**146**	48	134	134	143	135	98	58
		RX	484	13	0	0	290	0	0	0	**240**	84	220	220	234	222	162	94
tw-giftideas	5	F	**5**	59	0	0	58	0	0	0	**83**	32	52	52	**83**	52	75	19
		O	3 694	47	0	0	71	0	0	0	**2 189**	1 875	2 023	2 023	2 108	2 023	2 020	1 543
		T	**20**	62	0	0	68	0	0	0	**17 513**	7 165	13 578	13 578	**17 513**	13 578	15 479	5 140
		R25	268	48	0	0	87	0	0	0	**104**	67	76	76	98	76	88	37
		R50	314	58	0	0	92	0	0	0	**79**	52	59	59	75	59	69	29
		R75	210	47	0	0	**87**	0	0	0	**47**	31	34	34	**47**	34	39	16
		RX	164	43	0	0	85	0	0	0	**77**	51	58	58	75	58	66	27
	10	F	**16**	60	0	0	121	0	0	0	**128**	49	88	88	**128**	95	**128**	31
		O	432	60	0	0	154	0	0	0	**2 511**	2 219	2 224	2 224	2 292	2 266	2 304	1 761
		T	**112**	61	0	0	130	0	0	0	**29 047**	11 260	23 737	23 737	**29 047**	25 258	28 644	8 599
		R25	278	45	0	0	**178**	0	0	0	**168**	102	121	121	**168**	134	156	57
		R50	**153**	47	0	0	181	0	0	0	**128**	78	93	93	**128**	102	119	44
		R75	96	46	0	0	**180**	0	0	0	**78**	47	55	55	**78**	61	72	26
		RX	170	42	0	0	177	0	0	0	**126**	78	92	92	125	99	115	42
	15	F	**34**	58	0	0	182	0	0	0	**163**	87	127	127	**163**	131	159	74
		O	139	58	0	0	231	0	0	0	**2 646**	2 445	2 354	2 354	2 409	2 359	2 432	2 177
		T	352	48	0	0	**180**	0	0	0	**37 961**	21 708	34 308	34 308	**37 961**	34 697	36 612	19 099
		R25	278	49	0	0	271	0	0	0	**212**	147	168	168	210	173	193	115
		R50	232	47	0	0	276	0	0	0	**162**	112	129	129	161	131	147	88
		R75	169	46	0	0	273	0	0	0	**100**	69	78	78	99	80	89	51
		RX	419	42	0	0	274	0	0	0	**161**	114	126	126	159	129	144	85

Table 4: Runtimes and objective values for instances tw-greenenergy, tw-naturelovers, and tw-organicfood.

			runtimes								objective values							
Instance	$\|S\|$	Metric	GB	BC	DC	ED	MG	PR	RM	TR	GB	BC	DC	ED	MG	PR	RM	TR
tw-greenenergy	5	F	**1**	4	0	0	23	0	0	0	**19**	3	9	9	**19**	10	15	5
		O	383	4	0	0	32	0	0	0	**1 046**	426	930	930	930	880	735	373
		T	1	4	**0**	**0**	23	**0**	0	0	**1 886**	493	**1 886**	**1 886**	**1 886**	**1 886**	990	644
		R25	165	4	0	0	**34**	0	0	0	**94**	30	83	83	**94**	80	60	37
		R50	78	4	0	0	**36**	0	0	0	**76**	24	66	66	**76**	65	45	31
		R75	44	4	0	0	**35**	0	0	0	**53**	17	43	43	**53**	43	31	20
		RX	50	4	0	0	**34**	0	0	0	**77**	24	67	67	**77**	65	47	32
	10	F	**1**	4	0	0	46	0	0	0	**31**	6	19	19	**31**	18	22	5
		O	746	4	0	0	59	0	0	0	**1 342**	548	1 188	1 188	1 188	1 141	911	384
		T	2	4	**0**	**0**	47	**0**	0	0	**3 229**	800	**3 229**	**3 229**	**3 229**	3 199	1 668	980
		R25	203	4	0	0	73	0	0	0	**151**	42	135	135	150	132	78	42
		R50	144	4	0	0	**75**	0	0	0	**120**	35	104	104	**120**	104	60	35
		R75	117	4	0	0	**73**	0	0	0	**83**	25	71	71	**83**	70	41	23
		RX	90	4	0	0	73	0	0	0	**123**	35	108	108	120	106	63	37
	15	F	**2**	4	0	0	69	0	0	0	**40**	9	22	22	**40**	22	27	8
		O	926	4	0	0	87	0	0	0	**1 504**	813	1 276	1 276	1 276	1 276	1 007	495
		T	10	5	**0**	**0**	76	**0**	0	0	**4 307**	1 307	**4 307**	**4 307**	**4 307**	**4 307**	2 123	1 307
		R25	147	4	0	0	**112**	0	0	0	**192**	66	165	165	**192**	165	95	58
		R50	249	4	0	0	113	0	0	0	**151**	56	129	129	149	129	74	48
		R75	225	4	0	0	118	0	0	0	**106**	36	87	87	104	87	50	34
		RX	207	4	0	0	110	0	0	0	**155**	54	134	134	154	134	78	51
tw-naturelovers	5	F	**7**	355	0	0	572	2	0	0	**62**	34	53	53	**62**	31	60	51
		O	6 961	330	0	0	684	1	0	0	**7 105**	6 330	6 875	6 875	6 875	3 568	5 701	5 741
		T	**17**	372	0	0	599	2	0	0	**18 699**	12 441	16 757	16 757	**18 699**	14 075	14 487	11 757
		R25	**543**	348	0	0	840	1	0	0	**362**	268	314	314	**362**	98	183	264
		R50	**270**	359	0	0	850	2	0	0	**278**	201	232	232	**278**	78	138	198
		R75	**372**	436	0	0	868	2	0	0	**170**	122	142	142	**170**	46	81	124
		RX	**321**	301	0	0	830	1	0	0	**295**	213	251	251	**295**	77	144	210
	10	F	**24**	360	0	0	1 190	2	0	0	**114**	56	92	92	**114**	53	111	74
		O	7 189	336	0	0	1 392	2	0	0	**8 342**	7 173	7 847	7 847	7 828	4 254	7 016	7 241
		T	**110**	335	0	0	1 132	1	0	0	**33 147**	19 763	29 227	29 227	**33 147**	24 658	27 733	21 470
		R25	**645**	356	0	0	1 754	2	0	0	**551**	338	472	472	**551**	162	314	377
		R50	**559**	365	0	0	1 760	2	0	0	**421**	252	359	359	**421**	121	236	282
		R75	**314**	353	0	0	1 765	2	0	0	**265**	155	220	220	**265**	75	145	177
		RX	419	300	0	0	1 730	2	0	0	**447**	266	378	378	443	123	240	297
	15	F	**98**	391	0	0	2 010	2	0	0	**155**	69	137	137	**155**	70	144	96
		O	7 190	337	0	0	2 099	2	0	0	**9 063**	7 599	8 593	8 593	8 321	4 475	7 336	8 183
		T	**297**	330	0	0	1 704	1	0	0	**46 125**	24 480	42 152	42 152	**46 125**	33 377	38 169	30 214
		R25	789	388	0	0	2 699	2	0	0	**694**	398	606	606	691	200	385	508
		R50	645	357	0	0	2 686	2	0	0	**530**	297	459	459	529	151	286	378
		R75	696	359	0	0	2 689	2	0	0	**334**	184	285	285	331	94	178	239
		RX	432	297	0	0	2 634	1	0	0	**560**	314	482	482	558	153	295	403
tw-organicfood	5	F	**1**	0	0	0	**1**	0	0	0	**8**	1	5	5	**8**	5	6	0
		O	3	0	0	0	1	0	0	0	**82**	42	62	62	76	62	62	17
		T	**1**	0	0	0	**1**	0	0	0	**150**	61	140	140	**150**	140	129	24
		R25	46	0	0	0	**1**	0	0	0	**11**	5	9	9	**11**	9	8	3
		R50	56	0	0	0	1	0	0	0	**9**	4	7	7	8	7	6	1
		R75	33	0	0	0	**1**	0	0	0	**6**	3	4	4	**6**	4	4	2
		RX	13	0	0	0	1	0	0	0	**11**	6	8	8	10	8	8	2
	10	F	**1**	0	0	0	**1**	0	0	0	**11**	1	4	4	**11**	4	5	1
		O	7	0	0	0	1	0	0	0	**115**	59	63	63	89	63	58	19
		T	6	0	0	0	**1**	0	0	0	**217**	101	176	176	**217**	176	146	33
		R25	7 201	0	0	0	**2**	0	0	0	**17**	10	10	10	**17**	10	8	4
		R50	73	0	0	0	**2**	0	0	0	**14**	7	8	8	**14**	8	6	2
		R75	44	0	0	0	**2**	0	0	0	**10**	5	5	5	**10**	5	5	2
		RX	95	0	0	0	1	0	0	0	**16**	10	9	9	15	9	8	3
	15	F	9	0	0	0	**2**	0	0	0	**13**	2	4	4	**13**	4	5	1
		O	11	0	0	0	2	0	0	0	**134**	67	78	78	99	78	80	20
		T	8	0	0	0	**2**	0	0	0	**265**	125	217	217	**265**	217	178	44
		R25	7 202	0	0	0	3	0	0	0	**22**	13	14	14	21	14	12	4
		R50	210	0	0	0	3	0	0	0	**18**	9	11	11	17	11	11	2
		R75	117	0	0	0	**2**	0	0	0	**13**	7	7	7	**13**	7	7	2
		RX	1 156	0	0	0	3	0	0	0	**20**	12	13	13	19	13	12	3

Table 5: Runtimes and objective values for instances tw-orms, tw-skateboarding, and tw-travelling.

			runtimes								objective values							
Instance	$\|S\|$	Metric	GB	BC	DC	ED	MG	PR	RM	TR	GB	BC	DC	ED	MG	PR	RM	TR
tw-orms	5	F	**0**	0	0	0	1	0	0	0	**19**	13	18	11	**19**	18	14	6
		O	3	1	0	0	1	0	0	0	**217**	166	196	184	213	196	170	94
		T	2	0	0	0	**1**	0	0	0	**358**	266	334	344	**358**	334	247	115
		R25	15	0	0	0	**2**	0	0	0	**22**	16	20	18	**22**	20	17	9
		R50	25	1	0	0	**1**	0	0	0	**17**	12	15	15	**17**	15	13	6
		R75	9	0	0	0	**2**	0	0	0	**12**	8	10	10	**12**	10	9	5
		RX	7	0	0	0	**1**	0	0	0	**17**	12	15	14	**17**	15	14	7
	10	F	**1**	0	0	0	2	0	0	0	**29**	21	24	21	**29**	24	23	9
		O	8	0	0	0	3	0	0	0	**272**	211	254	244	253	254	242	140
		T	13	0	0	**0**	2	0	0	0	**556**	386	528	**556**	552	528	441	212
		R25	60	0	0	0	**3**	0	0	0	**34**	24	31	31	**34**	31	28	14
		R50	56	0	0	0	**3**	0	0	0	**26**	17	24	24	**26**	24	21	11
		R75	164	0	0	0	**3**	0	0	0	**18**	12	17	17	**18**	17	15	8
		RX	201	0	0	0	**3**	0	0	0	**25**	17	23	24	**25**	23	22	12
	15	F	**2**	0	0	0	3	0	0	0	**34**	24	29	25	**34**	29	25	11
		O	9	0	0	0	3	0	0	0	**302**	239	272	269	285	272	250	162
		T	43	0	0	0	2	0	0	0	**698**	488	673	690	694	673	480	260
		R25	265	0	0	0	5	0	0	0	**43**	30	39	39	42	39	31	16
		R50	280	0	0	0	**5**	0	0	0	**32**	22	29	29	**32**	29	23	12
		R75	1 478	0	0	0	5	0	0	0	**23**	16	21	21	22	21	16	9
		RX	748	0	0	0	**4**	0	0	0	**31**	21	29	29	**31**	29	23	14
tw-skateboarding	5	F	**3**	3	0	0	20	0	0	0	**41**	13	37	37	**41**	37	37	39
		O	13	2	0	0	24	0	0	0	**1 292**	670	1 247	1 247	1 247	1 247	1 169	973
		T	1	2	**0**	**0**	19	**0**	0	0	**2 705**	1 021	**2 705**	**2 705**	**2 705**	**2 705**	2 596	2 468
		R25	**17**	2	0	0	29	0	0	0	**160**	59	156	156	**160**	156	144	126
		R50	**14**	2	0	0	29	0	0	0	**120**	43	118	118	**120**	118	108	93
		R75	**10**	2	0	0	29	0	0	0	**82**	30	80	80	**82**	80	75	65
		RX	**14**	2	0	0	27	0	0	0	**131**	44	127	127	**131**	127	117	100
	10	F	**10**	2	0	0	39	0	0	0	**54**	23	52	53	**54**	52	49	51
		O	44	2	0	0	51	0	0	0	**1 495**	953	1 410	1 414	1 414	1 419	1 290	1 353
		T	2	3	0	**0**	44	0	0	0	**4 304**	2 066	4 192	**4 304**	**4 304**	4 204	3 634	3 931
		R25	79	3	0	0	**64**	0	0	0	**223**	106	215	218	**223**	218	184	202
		R50	**60**	2	0	0	63	0	0	0	**170**	75	163	164	**170**	163	139	152
		R75	**43**	2	0	0	63	0	0	0	**117**	53	113	114	**117**	113	97	104
		RX	53	2	0	0	57	0	0	0	**185**	80	178	180	184	178	150	162
	15	F	**14**	2	0	0	59	0	0	0	**64**	24	60	57	**64**	60	54	59
		O	64	2	0	0	75	0	0	0	**1 606**	995	1 472	1 470	1 494	1 458	1 389	1 438
		T	**12**	3	0	0	64	0	0	0	**5 466**	2 200	5 413	5 402	**5 466**	5 358	4 127	4 951
		R25	126	2	0	0	**95**	0	0	0	**265**	114	250	248	**265**	245	209	235
		R50	116	2	0	0	95	0	0	0	**203**	81	190	188	202	185	158	177
		R75	**71**	2	0	0	95	0	0	0	**141**	57	133	132	**141**	129	109	123
		RX	**68**	2	0	0	90	0	0	0	**220**	87	207	206	**220**	201	172	191
tw-travelling	5	F	**0**	1	0	0	7	0	0	0	**13**	5	3	3	**13**	5	5	1
		O	10	1	0	0	9	0	0	0	**389**	202	304	314	345	304	218	193
		T	**1**	1	0	0	7	0	0	0	**584**	257	507	576	**584**	507	343	209
		R25	42	1	0	0	**10**	0	0	0	**49**	15	37	39	**49**	37	21	20
		R50	23	1	0	0	11	0	0	0	**37**	12	27	28	35	27	14	15
		R75	**7**	1	0	0	11	0	0	0	**28**	6	18	19	**28**	18	9	11
		RX	22	1	0	0	**10**	0	0	0	**39**	10	25	27	**39**	25	15	17
	10	F	**0**	1	0	0	14	0	0	0	**19**	5	7	7	**19**	7	12	3
		O	142	1	0	0	19	0	0	0	**489**	253	414	409	423	414	307	216
		T	**12**	1	0	0	14	0	0	0	**1 017**	427	964	1 011	**1 017**	964	585	241
		R25	239	1	0	0	22	0	0	0	**76**	22	63	63	73	63	36	24
		R50	173	1	0	0	23	0	0	0	**56**	16	46	46	54	46	25	19
		R75	96	1	0	0	**22**	0	0	0	**40**	9	32	32	**40**	32	16	13
		RX	36	1	0	0	21	0	0	0	**60**	16	46	46	58	46	24	19
	15	F	**1**	1	0	0	22	0	0	0	**25**	7	9	8	**25**	9	13	3
		O	256	1	0	0	28	0	0	0	**550**	296	487	485	501	487	339	218
		T	29	1	0	0	**22**	0	0	0	**1 360**	563	1 325	1 352	**1 360**	1 325	702	261
		R25	245	1	0	0	34	0	0	0	**94**	30	86	84	93	86	42	25
		R50	227	1	0	0	34	0	0	0	**70**	22	63	63	69	63	29	19
		R75	153	1	0	0	34	0	0	0	**50**	13	45	45	49	45	20	13
		RX	83	1	0	0	31	0	0	0	**73**	22	65	65	72	65	30	20

Table 6: Runtimes and objective values for instances msg-college and msg-email-eu.

Instance	$\|S\|$	Metric	runtimes								objective values							
			GB	BC	DC	ED	MG	PR	RM	TR	GB	BC	DC	ED	MG	PR	RM	TR
msg-college	5	F	**2**	5	0	0	9	0	-	-	**7**	4	4	5	**7**	4	-	-
		O	**1**	4	0	0	12	0	-	-	**63**	54	57	58	**63**	55	-	-
		T	**1**	4	0	0	9	0	-	-	**65**	55	59	60	**65**	57	-	-
		R25	18	4	**0**	**0**	12	0	-	-	**4**	3	**4**	**4**	**4**	3	-	-
		R50	16	4	**0**	**0**	12	**0**	-	-	**3**	**3**	**3**	**3**	**3**	2	-	-
		R75	15	4	**0**	**0**	12	**0**	-	-	**2**	**2**	**2**	**2**	**2**	**2**	-	-
		RX	17	4	**0**	**0**	12	**0**	-	-	**3**	**3**	**3**	**3**	**3**	**3**	-	-
	10	F	**2**	4	0	0	18	0	-	-	**12**	8	8	8	**12**	8	-	-
		O	**5**	4	0	0	23	0	-	-	**103**	98	98	98	**103**	96	-	-
		T	**9**	5	0	0	21	0	-	-	**109**	103	103	103	**109**	101	-	-
		R25	48	4	**0**	**0**	25	**0**	-	-	**6**	**6**	**6**	**6**	**6**	**6**	-	-
		R50	53	4	**0**	**0**	25	0	-	-	**5**	**5**	**5**	**5**	**5**	4	-	-
		R75	28	4	**0**	**0**	25	**0**	-	-	**3**	**3**	**3**	**3**	**3**	**3**	-	-
		RX	54	4	**0**	**0**	25	**0**	-	-	**5**	**5**	**5**	**5**	**5**	**5**	-	-
	15	F	**5**	4	0	0	28	0	-	-	**15**	10	10	10	**15**	11	-	-
		O	**11**	4	0	0	35	0	-	-	**134**	128	129	129	**134**	128	-	-
		T	**27**	4	0	0	28	0	-	-	**145**	137	138	138	**145**	137	-	-
		R25	215	4	**0**	**0**	38	0	-	-	**8**	**8**	**8**	**8**	**8**	7	-	-
		R50	83	4	**0**	**0**	38	**0**	-	-	**6**	**6**	**6**	**6**	**6**	**6**	-	-
		R75	33	5	**0**	**0**	42	**0**	-	-	**4**	**4**	**4**	**4**	**4**	**4**	-	-
		RX	54	4	0	0	**38**	0	-	-	**7**	6	6	6	**7**	6	-	-
msg-email-eu	5	F	**1**	2	0	0	3	0	-	-	**8**	5	5	5	**8**	5	-	-
		O	**2**	2	0	0	4	0	-	-	**72**	61	66	66	**72**	66	-	-
		T	**2**	2	0	0	3	0	-	-	**78**	65	71	71	**78**	71	-	-
		R25	13	2	**0**	**0**	4	**0**	-	-	**2**	**2**	**2**	**2**	**2**	**2**	-	-
		R50	10	2	**0**	**0**	4	**0**	-	-	**1**	**1**	**1**	**1**	**1**	**1**	-	-
		R75	36	2	**0**	**0**	4	**0**	-	-	**1**	**1**	**1**	**1**	**1**	**1**	-	-
		RX	8	2	**0**	**0**	3	**0**	-	-	**1**	**1**	**1**	**1**	**1**	**1**	-	-
	10	F	**2**	2	0	0	6	0	-	-	**14**	8	10	10	**14**	9	-	-
		O	**5**	2	0	0	7	0	-	-	**112**	99	108	108	**112**	105	-	-
		T	12	2	0	0	**6**	0	-	-	**129**	110	123	123	**129**	118	-	-
		R25	66	2	**0**	**0**	9	**0**	-	-	**3**	**3**	**3**	**3**	**3**	**3**	-	-
		R50	29	2	**0**	**0**	8	**0**	-	-	**2**	**2**	**2**	**2**	**2**	**2**	-	-
		R75	914	2	**0**	**0**	8	**0**	-	-	**1**	**1**	**1**	**1**	**1**	**1**	-	-
		RX	22	2	**0**	**0**	7	**0**	-	-	**2**	**2**	**2**	**2**	**2**	**2**	-	-
	15	F	**5**	2	0	0	8	0	-	-	**18**	12	13	14	**18**	12	-	-
		O	10	2	0	0	10	0	-	-	**141**	130	136	135	140	133	-	-
		T	48	2	0	0	**9**	0	-	-	**167**	152	159	160	**167**	156	-	-
		R25	679	2	**0**	**0**	13	**0**	-	-	**4**	**4**	**4**	**4**	**4**	**4**	-	-
		R50	93	2	**0**	**0**	12	**0**	-	-	**3**	**3**	**3**	**3**	**3**	**3**	-	-
		R75	1 648	2	**0**	**0**	12	**0**	-	-	**2**	**2**	**2**	**2**	**2**	**2**	-	-
		RX	117	2	**0**	**0**	11	**0**	-	-	**3**	**3**	**3**	**3**	**3**	**3**	-	-

Table 7: Runtimes and objective values for instances soc-advogato and soc-anybeat.

			runtimes								objective values							
Instance	$\|S\|$	Metric	GB	BC	DC	ED	MG	PR	RM	TR	GB	BC	DC	ED	MG	PR	RM	TR
		F	**2**	29	0	0	72	0	-	-	**11**	8	10	10	**11**	10	-	-
		O	2	34	**0**	**0**	96	0	-	-	**114**	89	**114**	**114**	**114**	113	-	-
		T	**2**	28	0	0	72	0	-	-	**118**	90	117	117	**118**	116	-	-
	5	R25	**28**	34	0	0	100	0	-	-	**8**	5	7	7	**8**	7	-	-
		R50	**22**	35	0	0	101	0	-	-	**6**	4	5	5	**6**	5	-	-
		R75	**20**	27	0	0	93	0	-	-	**4**	2	3	3	**4**	3	-	-
		RX	28	27	**0**	**0**	92	**0**	-	-	**6**	4	**6**	**6**	6	**6**	-	-
		F	**4**	26	0	0	145	0	-	-	**16**	12	13	13	**16**	13	-	-
		O	11	27	**0**	**0**	176	**0**	-	-	**152**	137	**152**	**152**	**152**	150	-	-
		T	15	28	**0**	**0**	146	0	-	-	**159**	142	**159**	**159**	**159**	157	-	-
soc-advogato	10	R25	**123**	35	0	0	208	0	-	-	**11**	8	10	9	**11**	9	-	-
		R50	**93**	34	0	0	206	0	-	-	**8**	6	7	7	**8**	7	-	-
		R75	**31**	28	0	0	194	0	-	-	**6**	4	5	4	**6**	5	-	-
		RX	**72**	27	0	0	192	0	-	-	**9**	7	8	7	**9**	7	-	-
		F	**7**	27	0	0	216	0	-	-	**21**	14	16	16	**21**	15	-	-
		O	**31**	28	0	0	269	0	-	-	**186**	163	184	184	**186**	176	-	-
		T	**50**	28	0	0	222	0	-	-	**197**	170	195	195	**197**	187	-	-
	15	R25	1 229	36	0	0	**321**	0	-	-	**13**	10	11	11	**13**	11	-	-
		R50	708	28	0	0	**257**	0	-	-	**10**	8	9	9	**10**	9	-	-
		R75	**155**	29	0	0	298	0	-	-	**7**	5	6	6	**7**	6	-	-
		RX	247	27	0	0	291	0	-	-	**11**	8	9	9	10	9	-	-
		F	**14**	177	0	0	474	0	-	-	**44**	40	41	41	**44**	41	-	-
		O	**11**	224	0	0	585	0	-	-	**488**	461	483	483	**488**	483	-	-
		T	**12**	226	0	0	499	0	-	-	**506**	472	499	499	**506**	499	-	-
	5	R25	**62**	220	0	0	596	0	-	-	**72**	70	68	68	**72**	68	-	-
		R50	**50**	219	0	0	595	0	-	-	**56**	54	53	53	**56**	53	-	-
		R75	**36**	224	0	0	598	0	-	-	**40**	39	38	38	**40**	38	-	-
		RX	**29**	159	0	0	564	0	-	-	**58**	56	55	55	**58**	55	-	-
		F	**32**	163	0	0	909	0	-	-	**58**	51	54	56	**58**	52	-	-
		O	**26**	213	0	0	1 073	0	-	-	**624**	594	617	620	**624**	600	-	-
		T	**47**	236	0	0	912	0	-	-	**659**	622	649	652	**659**	630	-	-
soc-anybeat	10	R25	243	215	0	**0**	1 230	0	-	-	**85**	83	84	**85**	**85**	83	-	-
		R50	201	226	0	0	1 227	0	-	-	**66**	64	65	65	65	64	-	-
		R75	80	227	**0**	**0**	1 230	0	-	-	**47**	46	**47**	**47**	**47**	46	-	-
		RX	66	160	0	**0**	1 164	0	-	-	**68**	66	67	**68**	**68**	66	-	-
		F	**71**	229	0	0	1 502	0	-	-	**67**	56	65	65	**67**	59	-	-
		O	**45**	168	0	0	1 584	0	-	-	**709**	639	706	706	**709**	669	-	-
		T	**111**	242	0	0	1 432	0	-	-	**764**	676	756	756	**764**	714	-	-
	15	R25	**305**	234	0	0	1 864	0	-	-	**93**	88	92	92	**93**	89	-	-
		R50	**196**	234	0	0	1 876	0	-	-	**72**	68	71	71	**72**	68	-	-
		R75	**161**	224	0	0	1 869	0	-	-	**52**	49	51	51	**52**	49	-	-
		RX	**102**	158	0	0	1 767	0	-	-	**74**	70	73	73	**74**	71	-	-

D The impact of different utilities in competitive influence maximization

We now discuss results of the CIMP variant of R discussed in Section 2.4. In particular we discuss the impact of different utilities perceived from content views triggered by the leader and the follower. The results discussed in this section were obtained using our variant R for 50% resistant nodes (R50) and using optimal leader seed sets $L_{\texttt{R50}}$ for $|L_{\texttt{R50}}| \in \{5, 10, 15\}$ that were pre-computed by assuming no competition. The base values for our comparison correspond to the objective values denoted by $\hat{\sigma}^{-\infty}_{\texttt{R50}}(L_{\texttt{R50}}, \hat{S}^{*}_{\texttt{R50}})$ that were obtained by considering $a_i := e^{\bar{a}_j} = e^{-\infty}$, for all $i \in V \setminus L$ so that $r_i^{\omega} = r_i$, for all $i \in V \setminus L$, $\omega \in \Omega$. In other words, content views triggered by the leader have no impact on a node's patronage. We then increase the utilities perceived from viewing the leader's content to $a_i = e^0$, for all $i \in V \setminus L$, i.e., nodes gain equal utility from impressions triggered by the leader and the follower. We further use $a_i \in \{e^1, e^2, e^3, e^4\}$, for all $i \in V \setminus L$, in which case the utility perceived from viewing the leader's content is larger than viewing content from the follower.

Figure 9 compares the objective values of the aforementioned settings relative to the base values in which impressions triggered by the leader had no impact, i.e., values

$$\frac{\hat{\sigma}^{a}_{\texttt{R50}}(L_{\texttt{R50}}, \hat{S}^{*}_{\texttt{R50}})}{\hat{\sigma}^{-\infty}_{\texttt{R50}}(L_{\texttt{R50}}, \hat{S}^{*}_{\texttt{R50}})}$$

are reported for $a \in \{e^0, e^1, \ldots, e^4\}$. We observe a large impact of the utility values under investigation. More precisely, the results show the difficulty of convincing individuals having strong preference for a substitute product. The effects are also notable if the perceived utilities from products of services are equal from both the leader and the follower. For more detailed results we refer to Table 8.

Figure 9: Impact of different utilities perceived from impressions triggered by the leader and the follower.

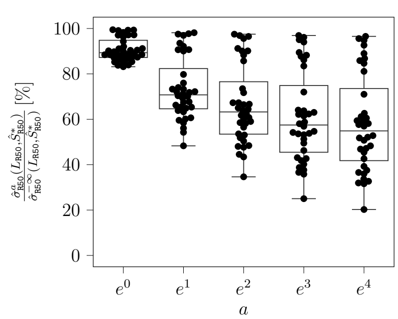

Note. The shown values are relative to values $\hat{\sigma}^{-\infty}_{\texttt{R50}}(L_{\texttt{R50}}, \hat{S}^{*}_{\texttt{R50}})$ obtained from solving the instances with $a_i = e^{-\infty}$, for all $i \in V \setminus L$, i.e., the case in which leader impressions have no impact at all.

Table 8: Runtimes and objective values for different utility values.

Instance	$\lvert L\rvert = \lvert S\rvert$	runtimes						objective values					
		$e^{-\infty}$	e^0	e^1	e^2	e^3	e^4	$e^{-\infty}$	e^0	e^1	e^2	e^3	e^4
	5	273	178	126	154	225	343	65	62	52	47	42	38
tw-austria	10	2 714	6 175	4 247	2 543	2 045	2 366	96	84	63	54	47	44
	15	6 721	3 195	888	5 004	7 201	7 201	119	104	76	64	55	51
	5	145	132	82	75	102	185	65	58	45	40	34	30
tw-giftideas	10	1 085	542	783	974	3 159	6 817	89	78	54	43	34	29
	15	7 198	6 879	4 260	6 197	7 195	7 200	106	89	59	47	38	33
	5	97	67	109	121	156	139	54	49	39	34	30	28
tw-greenenergy	10	511	302	191	294	391	400	71	62	48	41	36	33
	15	3 250	1 369	4 300	4 836	7 062	7 201	83	71	50	42	36	33
	5	836	463	404	386	584	767	176	159	125	110	95	85
tw-naturelovers	10	1 606	1 114	1 211	3 054	5 035	3 270	252	220	159	130	105	90
	15	5 511	4 841	5 830	5 968	7 188	7 190	293	250	174	142	113	96
	5	45	32	87	95	78	64	7	6	5	5	5	5
tw-organicfood	10	91	193	673	290	858	973	9	8	6	6	6	6
	15	2 175	1 200	4 589	7 201	7 201	7 201	10	9	7	7	7	6
	5	36	22	53	72	109	120	11	10	8	8	7	7
tw-orms	10	7 201	3 978	406	391	856	853	15	13	11	10	9	8
	15	4 641	2 463	376	169	482	314	17	15	11	10	9	9
	5	49	32	47	67	203	289	64	57	42	34	27	24
tw-skateboarding	10	262	171	153	357	2 777	5 973	81	69	47	39	32	30
	15	707	278	919	786	1 045	682	90	75	49	39	33	30
	5	104	100	102	79	67	80	22	21	16	15	14	13
tw-travelling	10	177	117	213	2 383	6 597	7 202	32	29	22	19	18	17
	15	7 202	7 201	7 201	7 203	7 203	6 778	33	28	21	19	18	17
	5	29	35	36	34	33	31	2	2	2	2	2	2
msg-college	10	105	116	76	82	93	111	3	3	3	3	3	3
	15	333	366	379	392	429	769	4	4	3	3	3	3
	5	16	16	14	14	15	16	1	1	1	1	1	1
msg-email-eu	10	1 005	571	400	442	466	612	1	1	1	1	1	1
	15	5 418	5 357	5 866	5 467	5 948	5 489	2	2	2	2	1	1
	5	69	69	70	73	74	79	2	2	2	2	2	2
soc-advogato	10	3 614	4 213	4 095	4 274	4 264	4 195	3	3	3	3	3	3
	15	7 199	7 199	7 199	7 199	7 199	7 200	4	4	4	4	4	4
	5	87	87	89	117	150	156	17	15	12	10	10	10
soc-anybeat	10	95	86	85	96	98	108	19	17	14	12	11	11
	15	2 699	2 644	1 853	1 868	1 607	2 430	50	42	24	17	13	10

E Instance plots

Figures 10 and 11 show (expected) in- and outdegrees of all instances used in this article. Notice that we removed two outlier nodes from instance soc-anybeat with outdegree $|\mathcal{N}(i)| > 1300$ and one node from instance tw-naturelovers with $|\mathcal{N}(i)| = 2910$ to enhance comparability.

Figure 10: Distribution of indegrees $|\mathcal{N}^-(i)|$ and outdegrees $|\mathcal{N}(i)|$ of used instances.

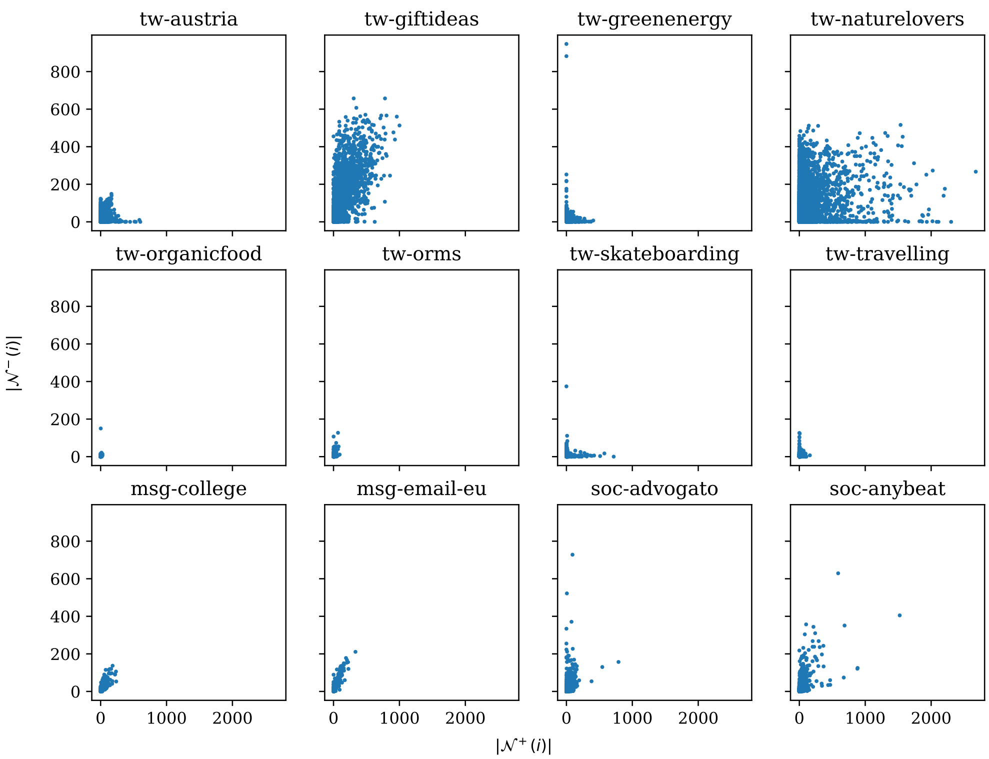

Figure 11: Distribution of expected indegrees $\mathbb{E}\left(|\mathcal{N}^{-}(i)|\right)$ and outdegrees $\mathbb{E}\left(|\mathcal{N}(i)|\right)$ of used instances.